A COMPUTER-DIRECTED SYSTEM FOR MEASURING DISTANCE BETWEEN EDGES IN OPTICAL IMAGES

Carl M. Shinn, Jr., et al

Washington University

Prepared for:

Advanced Research Projects Agency
Public Health Service

October 1968

DISCLAIMER NOTICE

THIS DOCUMENT IS THE BEST QUALITY AVAILABLE.

COPY FURNISHED CONTAINED A SIGNIFICANT NUMBER OF PAGES WHICH DO NOT REPRODUCE LEGIBLY.

Unclassified

Security Classification

AD-771 740 i

DOCUMENT CONTROL DATA - R & D

(Security classification of title, body of abstract and indexing annotation must be entered when the overall report is classified)

1 ORIGINATING ACTIVITY (Corporate author)	2a. REPORT SECURITY CLASSIFICATION
Computer Systems Laboratory Washington University St. Louis, Missouri	Unclassified
	2b. GROUP

3 REPORT TITLE

A Computer-Directed System for Measuring Distance between Edges in Optical Images

4. DESCRIPTIVE NOTES (Type of report and inclusive dates)

Interim

5. AUTHOR(S) (First name, middle initial, last name)

Carl M. Shinn, Jr. and Raymond M. Kline

6. REPORT DATE	7a. TOTAL NO. OF PAGES	7b. NO. OF REFS
October, 1968	~~80~~ 79	38

8a. CONTRACT OR GRANT NO.	9a. ORIGINATOR'S REPORT NUMBER(S)
(1) DOD(ARPA) Contract SD-302 (2) NIH(DRFR) Grant No. 00396 b. PROJECT NO. (1) ARPA Project Code No. 5880 c. Order No. 655 d.	Technical Report No. 10
	9b. OTHER REPORT NO(S) (Any other numbers that may be assigned this report)

10. DISTRIBUTION STATEMENT

Distribution of this document is unlimited.

11. SUPPLEMENTARY NOTES	12. SPONSORING MILITARY ACTIVITY
	ARPA - Information Processing Techniques Washington, D.C.NIH, Div. of Research

13. ABSTRACT

An automatic measuring system for time-varying optical images is described. After the operator specifies the location of the segment to be measured on an outline image produced by the system, the equipment periodically prints the current length on a teletype. A detailed study of optical edge detection by two different transformations is given. Finally tests of the system as a means of measuring and recording dynamic blood vessel diameters in the rat mesentery are explained.

DD FORM 1 NOV 68 1473 REPLACES DD FORM 1473, 1 JAN 64, WHICH IS OBSOLETE FOR ARMY USE.

Security Classification

14. KEY WORDS	LINK A		LINK B		LINK C	
	ROLE	WT	ROLE	WT	ROLE	WT
Automatic Measurement of Images						
Optical Edge Detection Transformations						
Dynamic Optical Measurements						
Vascular Diameter Measurements						
Outlining Transformations						
Image Processing						
Biological Microscopy						
Computer-directed Measurement System						
Image Dissector						
Laboratory INstrument Computer (LINC)						

ib

A COMPUTER-DIRECTED SYSTEM FOR MEASURING DISTANCE BETWEEN EDGES IN OPTICAL IMAGES

Carl M. Shinn, Jr. and Raymond M. Kline

TECHNICAL REPORT NO. 10

October, 1968

Computer Systems Laboratory

Washington University

St. Louis, Missouri

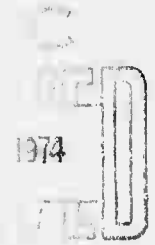

This work has been supported by the Advanced Research Projects Agency of the Department of Defense under contract SD-302 and by the Division of Research Facilities and Resources of the National Institutes of Health under Grant FR-00218.

"I often say that when you can measure what you are speaking about,
and express it in numbers, you know something about it:
but when you cannot express it in numbers,
your knowledge is of a meager and unsatisfactory kind...."

Lord Kelvin, 1883

ABSTRACT

An automatic measuring system for time-varying optical images is described. After the operator specifies the location of the segment to be measured on an outline image produced by the system, the equipment periodically prints the current length on a teletype. A detailed study of optical edge detection by two different transformations is given. Finally tests of the system as a means of measuring and recording dynamic blood vessel diameters in the rat mesentery are explained.

TABLE OF CONTENTS

No.		Page
1.	Introduction	1
	1.1 Objectives	1
	1.2 Literature Survey	2
	1.3 Image Processing System	5
2.	Theory of Image Outlines	9
	2.1 Producing Outlines by Differentiation	9
	2.2 Methods Used to Develop Outlines	10
	2.3 Preprocessing for Noise Minimization	13
3.	Outline Transformation Routines	22
	3.1 Introduction	22
	3.2 Outlining Transformation SS	23
	3.3 Outlining Transformation AC	29
	3.4 Comparison of Transformations SS and AC	30
4.	Auxiliary Routines	38
	4.1 Scan Manipulation	38
	4.1.1 Enlargement and Reduction	38
	4.1.2 Camera Field Map	39
	4.2 Intensity Monitoring	39
	4.2.1 Intensity Line Display and Histogram	41
	4.2.2 Contrast Enhancement	41
	4.3 Miscellaneous	44
	4.3.1 Calibration and Measurement Segment Indicator	44
	4.3.2 Parameter Printer	44
	4.3.3 Gray Level Image	46
	4.4 Measurement	46
5.	Results	54
	5.1 Outline Results	54
	5.2 Measurement Results	55
	5.3 Biological Results	62
6.	Summary, Conclusions, and Extensions	67
7.	Bibliography	68
8.	Acknowledgement	70

LIST OF TABLES

No.		Page
1.	Evaluation of Measurement Accuracy	59
2.	Evaluation of Measurement Consistency	61

LIST OF FIGURES

No.		Page
1.	Block Diagram of Image Processing System	6
2.	Photographs of the Equipment	7
3.	Effects of Noise on Edge Identification and Location	11
4.	Examples of Averaging Formats	14
5.	Error Minimization by Averaging	15
6.	Waveforms Demonstrating Effects of Increasing m (Points Average)	17
7.	Waveforms Demonstrating Effects of Increasing n (Spacing)	18
8.	Waveforms Demonstrating Advantages of Increased Spacing	19
9.	Intensity Profile for Micrometer Image Showing Effects of Increased Averaging	20
10.	Intensity Profile Where Transformation SS Detects Only One Edge	25
11.	Comparison of Thick Edges and Thin Edges Made of Transformation SS	26
12.	State Diagram for Transformation SS	27
13.	Flow Chart of Transformation SS	28
14.	State Diagram for Transformation AC	31
15.	Flow Chart of Transformation AC	32
16.	Intensity Profiles for Comparison of Transformations SS and AC	35
17.	Comparison of Bar Outlines Produced by Transformations SS and AC	36
18.	Influence of Thresholds on Outlines Produced by Transformation SS and AC	37
19.	Enlargement and Fast Window	40
20.	Intensity Line Display for Typical Line of Fly's Wing Image	42
21.	Typical Intensity Histogram	43
22.	Stage Micrometer Outlines, with Measurement and Calibration Indicators	45
23.	Parameter List Printed by Program on Teletype	47
24.	Flow Chart of Measurement Routine	48
25.	Flow Chart of MEASURE Subroutine	49
26.	Flow Chart of TIME AVERAGE Subroutine	50
27.	Flow Chart of SPACE AVERAGE Subroutine	52
28.	Halftone Picture with Outline Before Parameter Adjustment	56
29.	Outline Images Showing Parameter Changes	57
30.	Measurement Accuracy Test Pattern	58
31.	Halftone and Outline Images of Rat Mesentery	63
32.	Blood Vessel Outlines with Typical Intensity Line Display	64
33.	Blood Vessel Outlines with Measurement Segment	65

A COMPUTER-DIRECTED SYSTEM FOR MEASURING DISTANCE BETWEEN EDGES IN OPTICAL IMAGES

1. INTRODUCTION

Since the invention of the microscope, laboratory technicians have spent countless hours at the tedious task of making various measurements with that instrument. Lengths and areas under the microscope are of special interest in many metallurgical and biological problems. Direct visual measurement can be accomplished by inserting a calibrated scale or grid in the field of view and comparing the specimen to this reference. However, the difficulty involved in aligning the reference with the dimension to be measured and magnification of any motion in the field of view make accurate measurement by this method arduous and time-consuming, though certainly not impossible. Furthermore, it is almost impossible to make several measurements simultaneously by the traditional methods. Since speed and accuracy are the forte of the modern digital computer, this instrument may be reasonably expected to provide valuable aid in making microscopic measurements, or more generally, measurements on any optical image.

1.1 OBJECTIVES

A general purpose measurement device for optical images has many potential applications in biological microscopy (finding the size of cells, measuring distances between cells and between parts of cells, determining the length of dendrites), in metallurgy (calculating areas of phases by numerical integration), in aerial photography (measuring the distance between various physical features and man-made structures, finding areas covered by particular types of vegetation), and in other diverse fields. Such a system should be capable of swiftly computing the distance between any two object edges visible in an input image, as specified by an operator. This work demonstrates the versatility of an existing image processing system to serve as the vehicle for a general purpose optical measurement device. First the problem is explained and then previous efforts are summarized. In the last section of this chapter the existing image processing system is described.

What specifications should be given for a computer-directed measurement system for optical images? Interaction between the system and its human operator is an important consideration: on-line performance is desirable, particularly when the measured variable changes with time as in the example described below.

Results should be consistent as well as accurate, and they should be given in a convenient format. Suitable methods must be available to monitor the system and appropriate system parameters should be easy to adjust so that performance can be optimized.

A good test for such a device is dynamic blood vessel measurement. Blood vessel dia-

meters are known to be a function of the sympathetic nervous system activity and endogenous vasoactive substances in the blood stream. Physiologists have also injected various drugs into animals and observed the resulting dilations and/or constrictions of the animals' vessels. However, the vessel diameter reactions are often rather complex and hard to monitor for an extended interval of time. For instance, expansion of vessels on one side of the circulatory system (say, the arterial) may be coupled with simultaneous contraction on the other (venous) side. Also, immediate constriction may be followed by long-term dilation, or vice versa. More information on the mechanisms of capillary blood flow may be found in Chambers and Zweifach.[1]

Although much is known in a qualitative way about the effects of particular drugs, relatively little quantitative data has been obtained. Such quantitative data would, however, be of great benefit to physiologists. One method of investigating the reaction of blood vessels to a drug is by examining particular living arteries, veins, and capillaries through a microscope over a period of time after the injection. Linking a microscope with a computer-directed measurement system for optical images as envisioned above should furnish a way to acquire accurate vessel diameter data rapidly and easily. This work describes the development of an optical image measuring system and subsequent testing of the system as a means of measuring blood vessel diameters.

1.2 LITERATURE SURVEY

Many computer systems have been designed to expedite measurement of physical quantities: time, distance, pressure, temperature, chemical properties, and numerous other variables are swiftly and accurately recorded, even in environments hostile to man. Indeed, every pattern recognition system measures certain input variables in order to produce a decision, although the measurement may not be of the conventional variety. The endless variety of measuring systems precludes any exhaustive summary of all computerized mensuration schemes. Instead, some methods of making measurements on optical images with emphasis on microscopic biological subjects are described briefly.

Mann[2] gives an account of a system whose hardware is very similar to that presented in this work. (See section 1.3.) Although no measurements are recorded, the scheme makes use of a image dissector television camera and a small computer. Furthermore, the task is finding edges in the field of view, so one expects that finding the distance between these edges would not be a difficult extension of the program. While the particular application described is not length measurement, this example demonstrates the flexibility of a programmed image dissector.

Another digital picture processing system is titled Film Input to Digital Automatic Computer or FIDAC.[3,4] FIDAC consists of (a) a scanner which rapidly loads a picture from film into an IBM 7094 computer memory point by point and (b) the elaborate programs which can be called to operate on the digitized picture. The concept of choosing particular subroutines to process a given picture is appealing. This system is used in particular for pattern recognition studies (for e.g., analysis of photos of human chromosomes for variation that indicate genetic deficiencies.) Since FIDAC accepts only film input, it cannot function as a true on-line system because a roll of film must be developed before the information it contains can be put into the computer. Thus, dynamic measurements cannot be made automatically by FIDAC. Although speed is gained by processing picture points that have been previously stored in the memory, the convenience of the two-dimensional format in the image is lost.

Several examples are now cited to illustrate useful combinations of microscopes and various electronic scanning devices. A few of these instruments are available commercially, while the others are experimental equipment.

Commercially-available instruments include the Jarrell-Ash Quantimet,[5] which consists of a television camera and monitor, a microscope, and circuits for control and feature detection. A beam-splitter allows the operator to select the microscopic field of interest while the camera continuously scans the same field. Video output from the camera can be electronically analyzed by logic circuits to measure (a) percentage area occupied by features with density above or below a variable threshold, (b) number of intercepts of scan line with feature boundaries, (c) number of features in the field, and (d) size distribution of features. A disadvantage of the system for making linear length measurements is the lack of a means to select a single line from the raster for measurement. Nevertheless, the area fraction and average-length features are attractive for many metallurgical and biological applications.

Two measuring devices that are very similar in operation are manufactured by Airborne Instruments Laboratory. The AIL Type 490 Flying Spot Microscanner combines a flying spot scanner and a microscope,[6] whereas the AIL Type 491 Flying Spot Particle Analyzer applies the same scanner to photographic film.[7] These systems have about the same capabilities as the Jarrel-Ash system discussed above; however, the operator may also select a single line for study with the AIL instruments. All three commercial devices are somewhat inflexible; they can measure directly only in the scan line direction and they have fixed programs for making measurements. Therefore, they lack the versatility that is present in stored program equipment and which is highly desirable in a general purpose measurement system.

Another television microscope which uses the flying spot technique has been built in the U.S.S.R.[8] Instead of the electronically deflected beam used in most flying spot scanners, the Russian instrument has a high intensity light beam which is mechanically deflected by a system of mirrors; however, the transmitted light is collected into a photomultiplier tube just as in conventional scanners. The device is designed for biological studies, but its particular use at this time is not mentioned in the article, nor is any indication given that it has been used to automate length measurements. But the great potential advantages of using scanners and microscopes together are succintly summarized by these authors:

> The principle of line-by-line scanning in the formation of a television image alleviates the problem of extracting quantitative information from the image of a specimen. Observation of an oscillogram of a video signal extracted from a television raster makes it possible to judge the amount of light absorption by the specimen and the linear dimensions of the object that coincide with the scanning direction.[8, page 292]

Izzo and Coles have reported a highly specialized device for identifying rare blood cells which uses a vidicon television camera looking into a microscope.[9] While this tool quantizes the image of a cell into just two levels before further processing, the sequential "shrink" algorithm used to size cell parts is a good example of the sophistication made possible by digital procedures.

Other examples of microscopic scanner applications are given by Johnson et al.[10] and Warner and Brown.[11]

Next, another kind of measuring tool for minute images is summarized. An analog computer serves to measure distances along neural dendrites in a microscopic measuring system announced by Glaser and Van der Loos.[12] Endpoints are communicated to the system by means of a foot pedal. Between these coordinates (located in the field by means of crosshairs) all linear motions of the stage in X, Y, and Z are sent to the computer via transducers, and these

motions are integrated and summed in the computer to determine dendritic lengths by means of the Pythagorean theorem. While this procedure may sound slow and awkward compared to digital techniques, it is actually rather accurate and efficient. The slow semiautomatic operation is dictated by the complexity of the dendritic structure that the system is designed to measure.

The results perhaps most directly comparable to those to be described in this work are those reported by Wiederhielm.[13-15] Based on an idea originally suggested by Block,[16] Wiederhielm's arrangement consists of a vidicon camera looking into a microscope. A K-mirror system is provided to rotate blood vessel images so that they are normal to the raster scan direction for accurate measurement. Gating allows a single line to be selected from the raster for analysis; this line is marked (unblanked) in the monitor image and the video for the same line is recorded by an oscilloscope camera. In addition the same signal may be applied to another scope on which a history of the particular line is built up by recording the traces in sequence. Finally, the same video signal can be applied to a measuring circuit, which includes a Schmitt trigger that can be adjusted to trigger at any selected level on a waveform. In turn the trigger turns on a ramp generator at the leading edge of a vessel waveform and turns it off at the lagging edge. The peak amplitude reached by the generated ramp provides a convenient indication of the vessel width.

Measured vessel widths are utilized by an analog computer to calculate other variables of interest in Wiederhielm's system. All data, including vessel outer diameters as measured, are recorded by polygraph. Baez has developed a similar method by employing the concept of image-shearing, which claims accuracy better by a factor of ten or more than the resolving power of the optical system.[17,18]

Summarizing, the method of scanning a microscopic image with a storage-type television camera is attractive because quantitative information on densities and dimensions is easy to obtain from the electrical signals which are generated. The large monitor picture is also easier to see than a microscope image. Adding a computer to the television microscope allows rapid measurements to be made and recorded automatically.

However, various disadvantages of the systems above make them inadequate as general purpose measurement devices for optical images. Virtually all are confined to scanning a single type of input, i.e., either a microscope image or a film transparency, but not both. FIDAC and other film input systems suffer from the inability to scan on-line. The commercial instruments (Quantimet and the AIL scanners) are low in cost, but they lack versatility, as does the special tool described by Izzo and Coles. The Russian flying spot microscope is mechanical and therefore slow. Although the analog measuring system reported by Glaser and Van der Loos requires no image processing or interpretation by the computer (and so might be considered more reliable), it is also slow. While speed is not a primary requirement for all optical measuring instruments, it becomes important whenever several objects must be measured almost simultaneously, as in the case of pressure flow studies on blood vessels.

Wiederhielm's system permits only one object to be measured at once and it is also restricted to microscope images. Furthermore, the analog circuitry used to make the measurements is not as flexible as a digital computer program. The image-shearing device reported by Baez requires a trained operator and only fifteen measurements can be made with it in a minute.

Avoiding the disadvantages listed above, the system explained in this work is fast and flexible. Moreover, it can operate on-line and it can accept input from either a microscope or a transparency. Next, hardware aspects of the system are discussed briefly.

1.3 IMAGE PROCESSING SYSTEM

Making length measurements automatically with a digital computer requires that some kind of digital picture processing be performed first. A convenient way to describe this operation is to consider transformations made on a digitized picture by an image processing system. A digitized picture is a matrix of picture elements, each of which is defined by its row, its column, and its particular descriptive value. Such elements are called points throughout this work. Although many variables (for example, color, hue, contrast, etc.) can be associated with the points, only a finite range of intensity values is necessary in the following scheme. (The concept of intensity is used here instead of density because the latter word is more often connected with film, whereas microscope images must also be treated.) Rows of points are termed lines and a number of adjacent lines are called a picture or an image. Transformation of a given picture into another is accomplished by changing the value of each point in an input image to a new value according to some function. Although transformations often greatly alter the appearance of a picture, they can considerably improve it for measurement, pattern recognition, and other tasks.

Image processing systems may be easily described in terms of their components: (a) a scanner used to convert an optical image into signals (usually electrical) that are most convenient for the processor, (b) a processor, which performs the transformations mentioned earlier, as well as any additional data manipulations, such as pattern recognition or measurement, and (c) an output, which may consist of a display device for the transformed image or some device to record the classifications or measurements made by the system.

Figure 1 is a block diagram of the particular image processing system used in this study. Note that two kinds of input images are available. Transparent film may be placed against a panel fluorescent light source set in front of the camera or small specimens may be viewed under a microscope with the resulting enlarged image reflected into the camera by a front-surface mirror. The image dissector television camera serves as a scanner for both forms of input by converting the optical intensity at a particular point to a voltage signal which is sent to the LINC.

Coordination of the input and output operations as well as processing of the data is performed by programs in the LINC. Communications from the LINC to the other devices (such as X and Y deflection of the camera) are handled via digital-to-analog converters in the LINC, and analog intensity data flowing to the LINC from the image dissector enters via analog-to-digital converters in the LINC. The analog preprocessing circuit between the camera and the computer consists of amplifiers for gain and offset which allow conversion of camera output voltages to the range sampled by the LINC. A logarithmic amplifier is also included because optical intensities in a typical image cover many decades. This wide range means that if the linear amplifier is set so that it has a maximum output voltage corresponding to the maximum input intensity, several intensity decades at the dark end of the spectrum are compressed into a very small voltage difference. The logarithmic amplifier spreads each intensity decade over the same voltage increment.

Outputs from the system may include measurements and tabulated parameters on the teletype or images on either of two scopes. A Tektronix 561A Oscilloscope can be used to provide a halftone reproduction of the image as seen by the camera while a Tektronix 564 Storage Oscilloscope supplies a way to save two level (outline) pictures generated by the system. Finally the image produced by either scope may be observed directly by the operator or it may be recorded by means of a Polaroid scope camera.

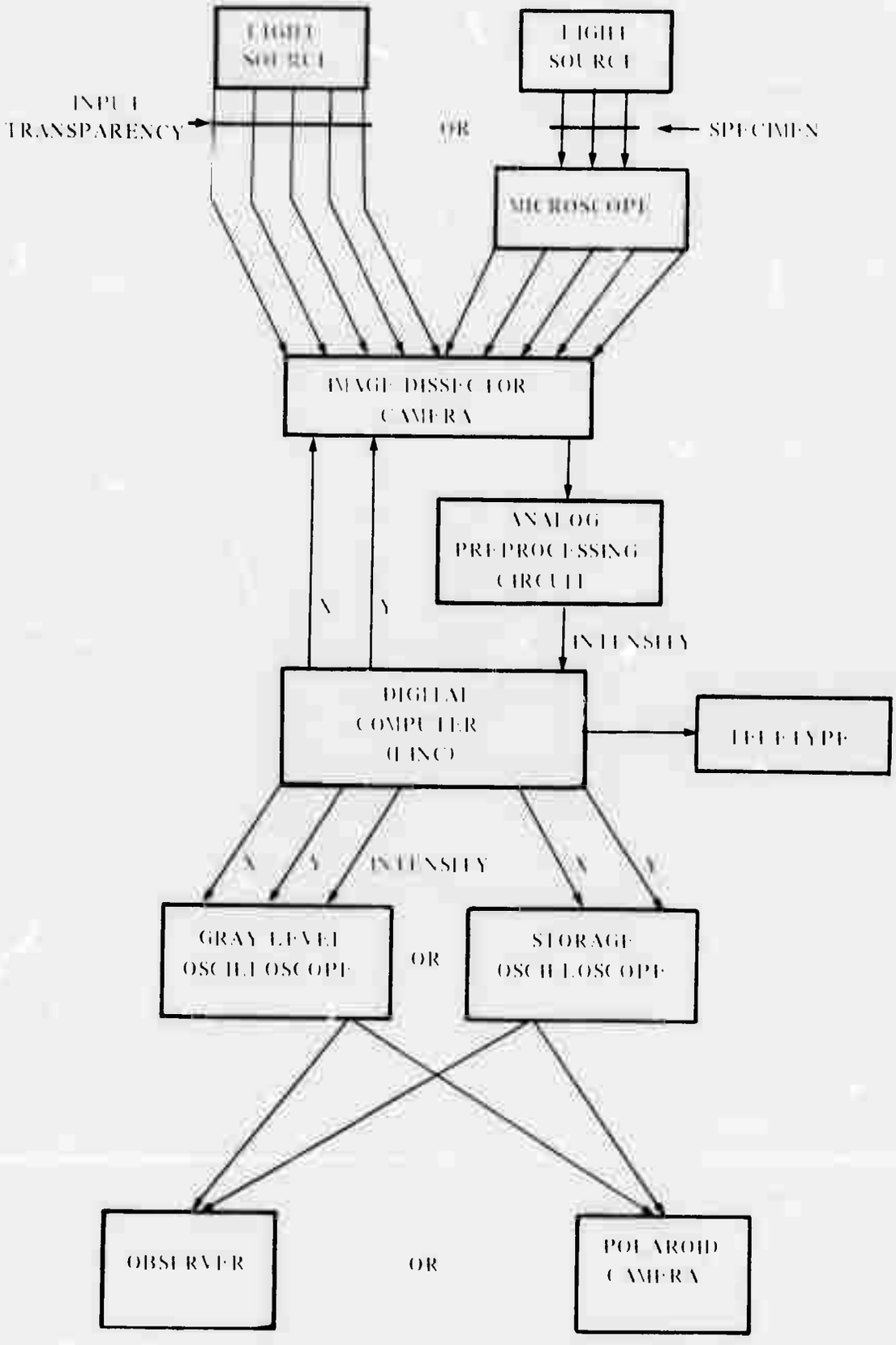

Figure 1. Block Diagram of Image Processing System

(a) Image Processing System with Light Source

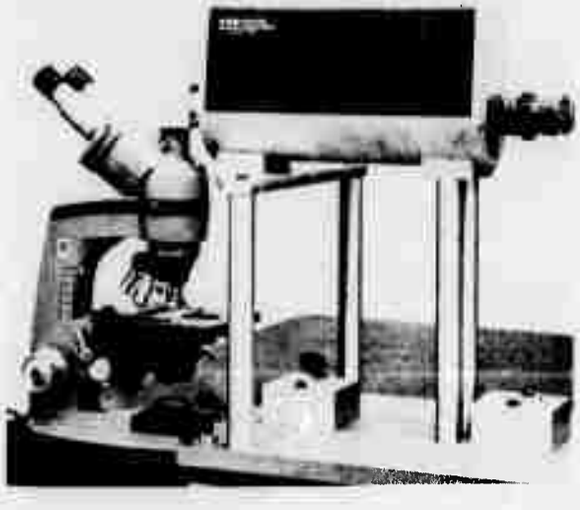

(b) Microscope and Image Dissector Television Camera

Figure 2. Photographs of the Equipment

Further details regarding the LINC may be found in the references.[19,20] Guignon and Kline[21] have previously described the image processing system.

The image processing system can be seen in Figure 2(a). On the table is the image dissector camera looking at the fluorescent light source. Under the table is the preprocessing equipment, and the LINC console as well as one of the display scopes are in the background. Figure 2(b) shows the microscope on the left with the camera looking into it from the right. The specimen may be observed through the binocular eyepieces on the left or a mirror inside the microscope can be turned to let the camera see the same image.

2. THEORY OF IMAGE OUTLINES

In many picture-processing applications some small portions of the copious data in an original image provides sufficient information for making the desired measurements or interpretations of the image. For example, the luxuriant colors present in a particular picture may be irrelevant to categorizing the textures in the image or to counting the number of objects in the scene. Perhaps the most obvious and the most important picture simplification for many purposes is the outline image, which displays only the edges present in the original.

Outlines become important whenever the edges of objects in an image supply the information to be processed. Counting objects, determining their dimensions (heights, widths, diameters, perimeters, or areas), ascertaining their shapes (as in identifying symbols or characters), and cataloging their relative locations represent examples of operations for which outlines contain ample input data. The measurements which are the subject of this work certainly may be obtained from suitable outline representations of the objects.

This chapter therefore discusses the general concept of producing outline pictures as well as some practical methods which have been suggested or utilized for that purpose. Also included is an elucidation of the digital preprocessing which conditions the input signals before the edge detection operations.

2.1 PRODUCING OUTLINES BY DIFFERENTIATION

Although seeing the outlines or contours of objects appears to be a sophisticated and important part of human visual perception, workers in the field of picture processing have apparently made little reference to the study of psychophysics. Thus, discussions of what constitutes a visual edge and how best to represent it in an outline picture are infrequent and inadequate. Perhaps worthy of future investigation is the observation by the great physicist Ernst Mach that the human eye emphasizes areas where there is a change in the rate of change of luminance with respect to distance.[22, page 217] While seeing machines cannot in the near future be expected to rival human visual perception in sophistication, and whereas there is some evidence that machines should *not* be built so as to perform their tasks in the same way that humans do, still there is interesting and useful work to be explored in this area of psychophysics. Gibson,[23] Attneave and Arnoult,[24] Hurvich and Jameson,[25] Graham,[26] and Attneave[27] have discussed this subject. Outside the field of psychophysics, interesting experiments have been performed by Higgins and Jones[28] to show the relationship between subjective judgments of the sharpness of a photograph and the acutance of the photographic material. Acutance is determined from the intensity-distance profile of a knife-blade image of the same material.

The term "edge" as used here refers to a boundary in an input image which divides a region of lesser density from a region of greater density. The goal of outline processing is to produce an essentially two-level (binary) picture in which one level accurately reproduces all such boundaries in the original and the other level serves as background. (Occasionally there may be applications which require several levels to yield various edge intensities.) It follows from this definition of an edge that the detection of edges in an input image in order to produce the corresponding outline image must involve a process of differentiation. Some form of differentiation of intensity or density with respect to distance in the image is required to locate edges, and the magnitude of this derivative gives some measure of how sharp the edge appears.

An inevitable difficulty associated with any differentiator is noise. Examples of noise associated with input images are noise voltage superimposed on the electrical signal representing the image and film grain noise associated with a photographic transparency of the image. Any deviation from the input signal is increased by the operation of differentiation.

The errors which can be introduced in the specific process of detecting outlines are demonstrated in Figure 3 where intensity increases upward on the vertical axis and distance along the scanned line increases toward the right on the horizontal axis. On the left (A and B) are examples of noise pulses and bursts which may be falsely identified as edges. The burst at C may cause the true edge, which should be placed at E_1, to be located at E_c. Likewise the noise labeled D makes edge E_2 appear steeper than it actually is. All these effects make it important to maximize the signal-to-noise ratio in an image processing system, especially when the outlines created are to be the input to a measuring routine.

After reducing the noise amplitude as much as possible by proper electronic design, several means can be used to further minimize the effects of the noise. A simple integration performed by arithmetically averaging several sampled intensities together suffices to diminish or eliminate some noise pulses. However, this operation also distorts real edge signals by reducing their steepness and amplitude. Another way to attenuate the influence of image noise is by using digital procedures to distinguish it from true edges; Chapter 3 will deal with some operations for this purpose.

2.2 METHODS USED TO DEVELOP OUTLINES

Numerous schemes have been proposed to allow generating outline images, and some representative examples are considered below in order to provide background for the system described later in this report. A distinction should be made between binary input pictures and multilevel image inputs. Although further transformations may be required to create binary outlines from a two-level input, the edges in the image are already inherently present. Nevertheless, brief examination of the outlining procedure for binary inputs reveals the nature of the problem and gives valuable insight into the multilevel case.

Brain et al.[29] have investigated photographic means of changing multilevel representations into two-level images. An example of these methods is the production of an outline photograph by using a defocused photographic positive in register with the negative of the same picture. Each of the methods described either tends to be inadequately sensitive to edges in the original or encounters difficulties due to photographic grain noise. Clarke[30] reports another photographic process which uses infrared radiation to quench luminescence at those positions where a negative lets light through. Although strikingly good outlines are produced by this process, methods employing sophisticated photography are not compatible with the on-line capabilities desired in the present applications.

Algorithms which generate a successful outline of objects in a binary input picture can be described in terms of the immediate neighbors (A, B, C, D, E, F, G, and H) of the cell labeled X in the diagram on the right.[31] If X* represents the contents of the cell X after the operation, then it can be described as

A	B	C
D	X	F
F	G	H

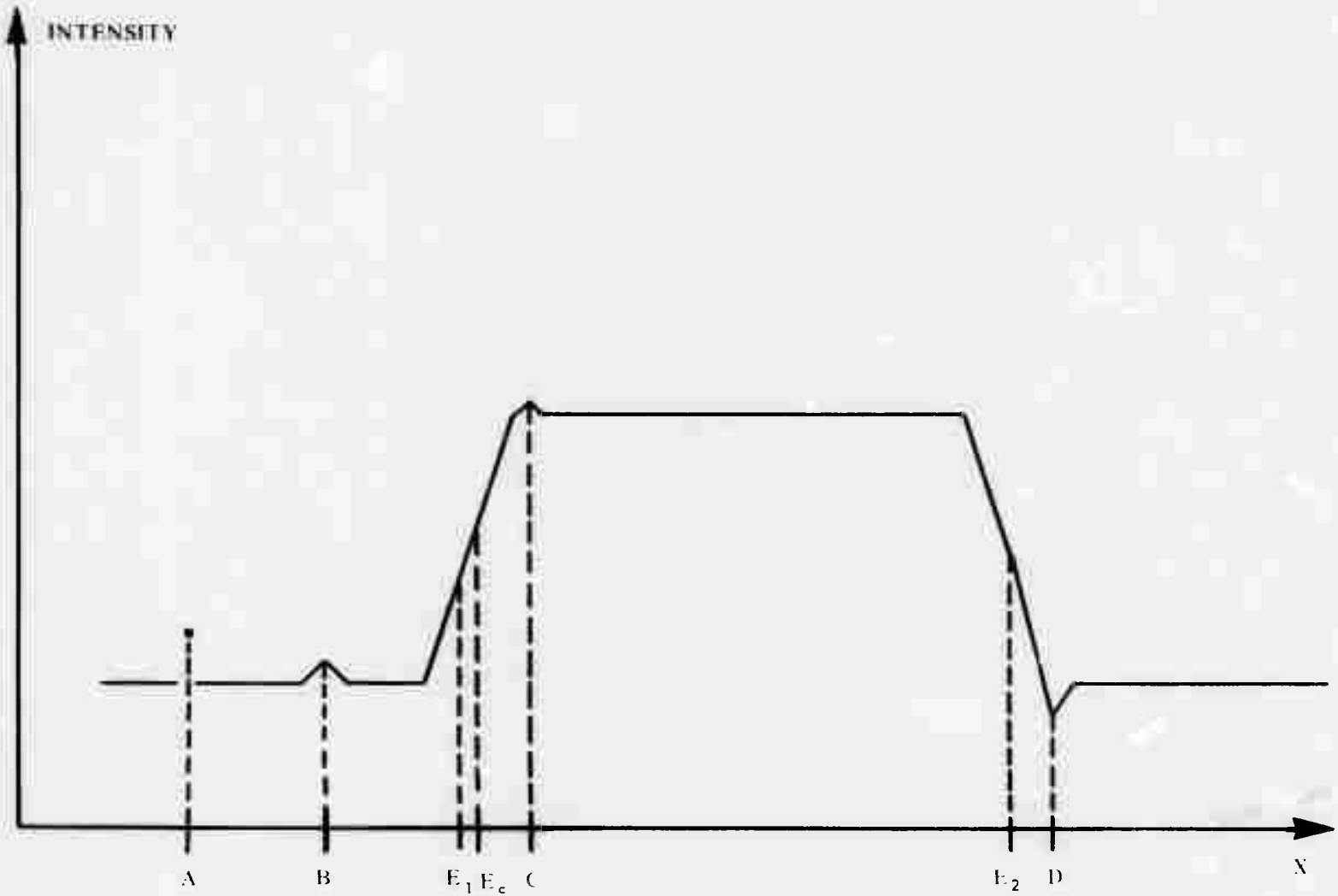

Figure 3. Effects of Noise on Edge Identification and Location

the Boolean function

$$X^* = X(A+B+C+D+E+F+G+H)$$

or slightly less accurately as

$$X^* = X(B+D+E+G)$$

Notice that these expressions yield symmetrical outlines with respect to the original image. However, they also propagate single isolated bits and chains of bits which represent very thin objects that should therefore not have well-defined outlines in a binary quantized space. Hence these algorithms illustrate some of the dilemmas intrinsic in the outlining process.

Binary edges have been traced or followed by Minot.[32] The procedure used involves serial scanning of the image until a black (object) cell is encountered. Then the program traces along the black-white edge, meanwhile watching for subtle cases of very thin edges, until the original edge cell is met again. This early work demonstrates several of the fundamental concepts associated with the problem of sequentially constructing outlines, such as the necessity for recognizing and handling properly "link" structures between larger areas and the subtleties of detecting edges enclosed by other edges.

Guignon[33] produced outline output images from multilevel input pictures using the same hardware, except for the microscope, that composes the present system. The basis of the procedure utilized is a two-dimensional intensity derivative approximation: the displayed intensity depends upon the intensity difference in the vertical direction and in the direction at forty-five degree from the vertical direction. That is, the intensity at any given point is subtracted from the intensity of the point at the same position in the previous line, and then it is subtracted from the intensity of the next point in the previous line. The greatest of these two absolute differences becomes the display intensity. Hence the displayed point has an intensity proportional to the magnitude of the edge, and both horizontal and vertical edges are effectively detected simultaneously. Advantages of such a scheme include an indication of how abrupt the edge is and a production of the outline image in a single raster scan, as compared with the programs described later in this work which differentiate only in a single direction and so require two complete raster scans in order to detect all edges in an input picture. However, measurement must take place in one direction only, so a scheme which finds edges simultaneously in two directions makes unidirectional measurement more difficult to implement.

One disadvantage of this method is a tendency to display dark gray points in regions where the intensity slowly varies without forming a true edge. Also, a multilevel display must be used: if the display is to be on-line as desired, an expensive multilevel storage scope is required. Moreover, no attempt is made to eliminate noise, and comparatively thick edges are displayed because several points are sampled on a typical edge scanned by the system.

Problems involving computer perception of three-dimensional solids led Roberts[34] to derive a new differential operator for detecting edges in pictures. Moreover, three criteria are listed which are important in judging the success of any edge-producing operation: (a) sharpness of the edge produced, (b) minimum background noise, and (c) edge intensity corresponding to the capacity of a human eye to detect the edge in the original image. Roberts comments that the number of samples used by the edge producing scheme determines the sharpness of an edge, that operators symmetric in the horizontal and vertical directions reduce the background noise, and that using the square root of the intensities in calculations yields correct edge intensities. Hence the functions he uses to find edges are described by the equations

$$y_{i,j} = \sqrt{x_{i,j}}$$

$$z_{i,j} = \sqrt{(y_{i,j} - y_{i+1,j+1})^2 + (y_{i+1,j} - y_{i,j+1})^2}$$

where $x_{i,j}$ is the initial intensity value of the point at the intersection of column i and row j and $z_{i,j}$ is the computed derivative value which is proportional to the probability of an edge through the point. Good results have been obtained by this method, but it requires use of a half-million bits of storage and extensive calculations which prohibit its use as an on-line measurement system except perhaps with large computers.

Images are processed as two separate components by Schreiber's synthetic highs system.[35] A low-pass filter yields a signal which describes the level in the original picture while at edges a differentiator supplies the signal which is digitized by an edge encoder. Considerable savings in the band width required to transmit an image can be realized with such a system, but for the problem of measurement described here, the level information is useless while the differential signal does not contain sufficient information to be useful without further processing.

Another elaborate scheme for detecting edges is the use of masks to compare the amount of light transmitted by adjacent areas of the original image.[36] Brain et al. produce 1024 replicas of an input image which are presented to 512 mask pairs, each of which allows light to pass through two small adjacent areas. If one mask of the pair allows considerably more light transmission than the other, then an edge is detected along the mutual boundary of the masks. By producing mask pairs whose mutual boundaries are centered at various positions in the image and are aligned at various angles with the horizontal, a meaningful selection of edges can be detected. Nevertheless, such a device cannot easily attain the resolution available through other systems and hence is better adapted to optical character recognition, for which it is currently used.

Summarizing, none of the procedures just described is completely suitable as a means to produce outlines which can form the basis for on-line measurements utilizing the present image processing system. Briefly, the primary disadvantage of each process for this application is now listed. Photographic film techniques are too slow and cumbersome to permit on-line processing. Because the specified input has many levels, binary methods are not directly applicable, although the concept of outlining can be neatly illustrated with two-level-input processors. Guignon's greatest-absolute-difference method is nearest to the required algorithm, but it does not produce sharp edges and it is inconvenient for measuring between edges because it detects edges in two directions at once. The functions Roberts utilizes are too slow for on-line processing with the LINC and also require more memory than is available. The Brain mask system and Schreiber's synthetic highs system are unnecessarily complicated for this application. Therefore, the techniques described in Chapter 3 are proposed. Some preprocessing of the input data is required, however, and this is explained next.

2.3 PREPROCESSING FOR NOISE MINIMIZATION

Difficulties imposed by noise have been described above. Various forms of arithmetic averaging were applied to the input signal in an effort to diminish the effects of this noise with a minimum-time operation. One unsatisfactory approach is to average together several samples from the same location in the image with the aim of reducing noise generated in the electronic circuitry. Although some reduction of noise is accomplished by this process, the

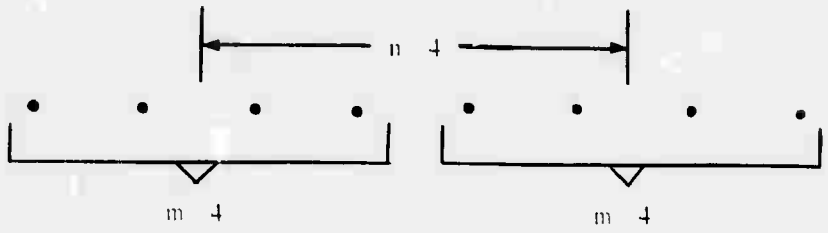

(a) 4x4 (4 points/average; spacing=4)

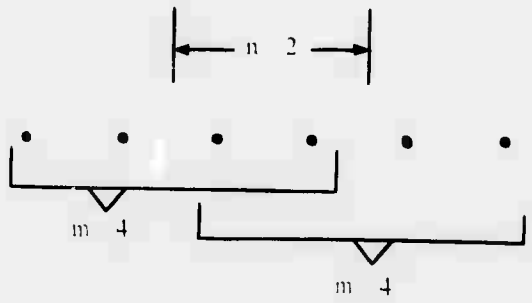

(b) 4x2 (4 points/average; spacing=2)

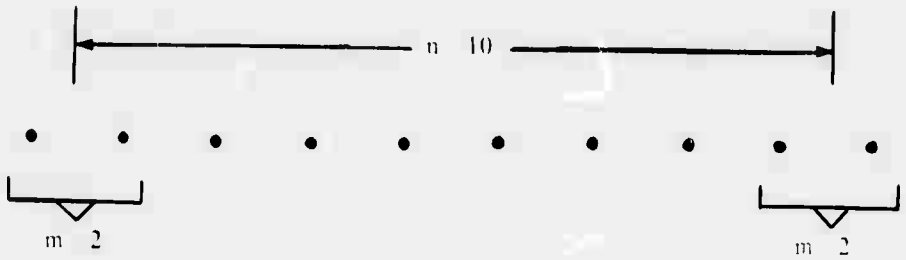

(c) 2x10 (2 points/average; spacing=10)

Figure 4. Examples of Averaging Formats

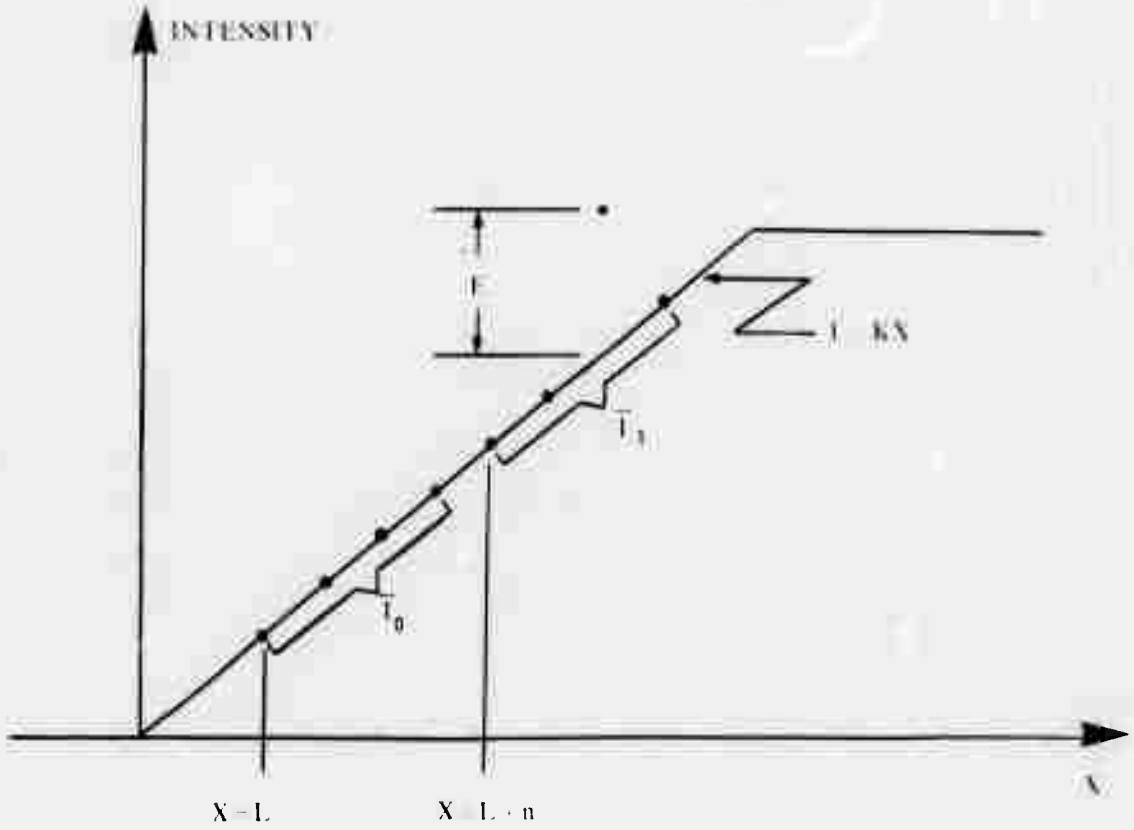

Figure 5. Error Minimization by Averaging

extra time necessary to perform it makes it undesirable. (Also some electrical integration by means of a filter is built into the preprocessing circuitry; while this method is faster than digital averaging, it does not eliminate all the noise.) Averaging several adjacent noisy input intensities together yields profitable smoothing, however, and this operation will now be discussed.

Important parameters of the type of averaging described here are (a) the number of points to be included in each average and (b) the spacing (also expressed as the number of points) from the center of one average to the center of the average with which it is to be compared. Both variables were assigned values in powers of two only in order to simplify their implementation in the computer programs. The advantage of the first parameter (points/average) is easily understood: the greater the number of points contributing to each intensity average, the smoother the processed waveform. The spacing, although perhaps not as obvious a variable as points/average, controls the amount of overlap of the averaged points, i.e., the number of points which contribute to both of the averaged points that determine the derivative at a particular location. For notational convenience the format m × n is used to refer to processing where m points are included in each average and n points separate the centers of averages which are compared. Note that m is always the first parameter used: spacing is determined after the averages have been calculated. In Figure 4 examples of the format can be studied. For instance, (a) illustrates the case where the averages compared have minimum spacing without overlapping, i.e., where m = n. In (b) the averages do overlap (m>n) while the averages in (c) are widely separated (m<n). Note that all numbers are given in octal.

In order to better understand the mechanics of this averaging, consider the truncated ramp shown in Figure 5. There are generally m points in an average and n points between averages, but m = n = 4 in the drawing in order to make the point more explicitly. Assume that the averages, $\bar{I}_0$ and $\bar{I}_1$, do not overlap so that only $\bar{I}_1$ includes a point in error by an amount E. Let $\bar{I}_0$ begin at x = L, so that $\bar{I}_1$ begins at x = L + n. Now the averages may be written as

$$\bar{I}_0 = \frac{KL+K(L+1)+\ldots+K(L+m-1)}{m}$$

and

$$\bar{I}_1 = \frac{K(L+n)+K(L+n+1)+\ldots+K(L+n+m-1)+E}{m}$$

Hence the derivative approximation is

$$\frac{\Delta I}{\Delta X} = \frac{\bar{I}_1-\bar{I}_0}{n}$$

$$= \frac{K(L+n)+K(L+n+1)+\ldots+K(L+n+m-1)+E-KL-K(L+1)-\ldots-K(L+m-1)}{mn}$$

$$= \frac{mKn+E}{mn}$$

$$= K + \frac{E}{mn}$$

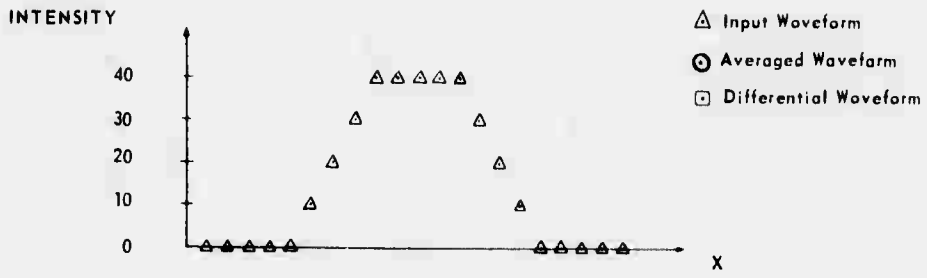

(a) Trapezoidal Input Waveform

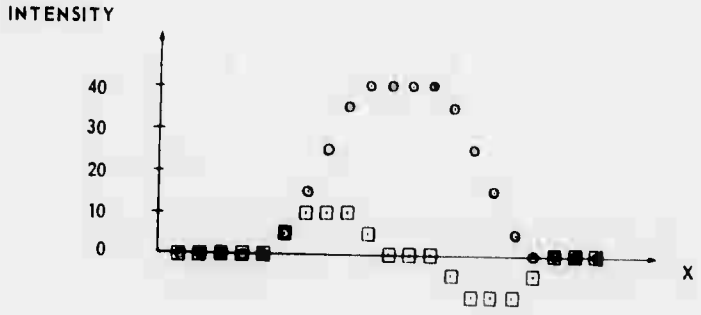

(b) Differential Waveform for m=2

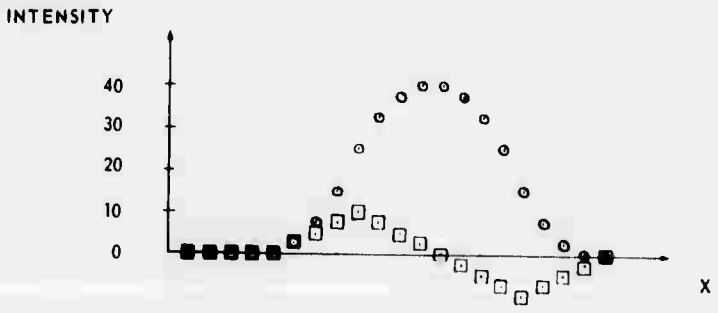

(c) Differential Waveform for m=4

Figure 6. Waveforms Demonstrating Effects of Increasing m (Points/Average)

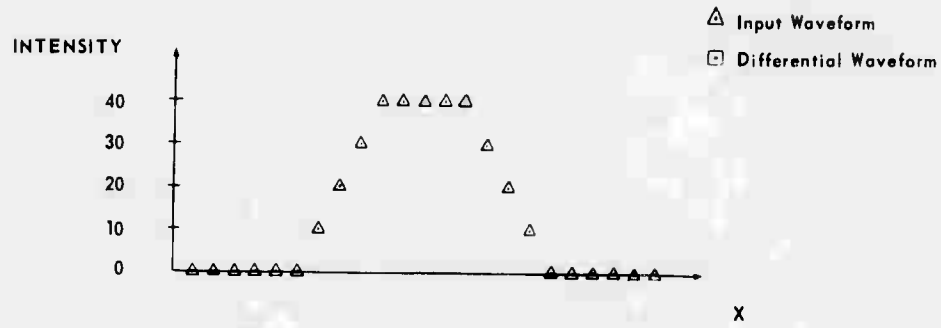

(a) Trapezoidal Input Waveform

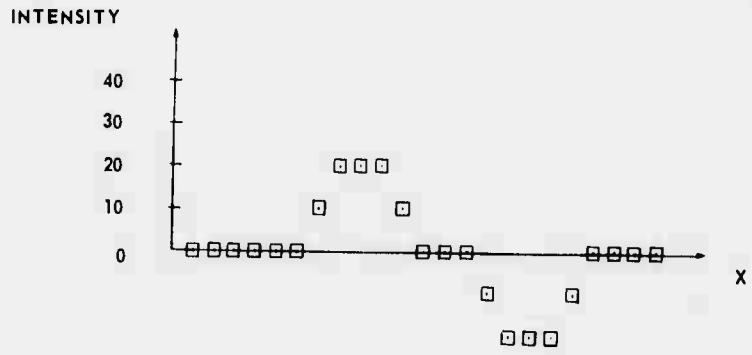

(b) Differential Waveform for n=2

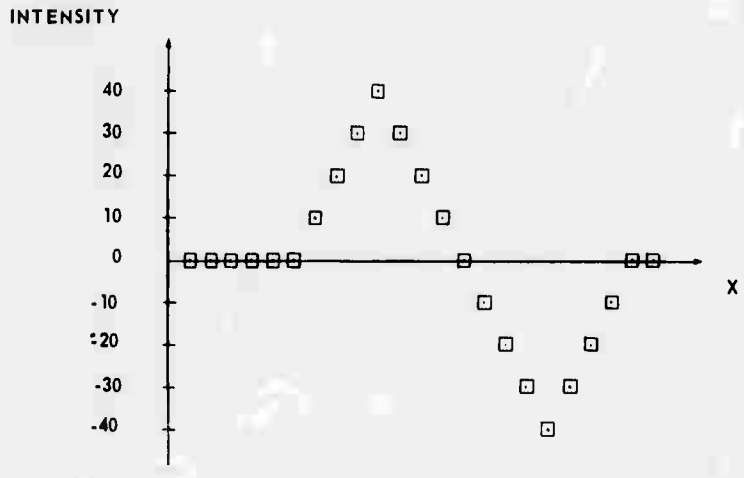

(c) Differential Waveform for n=4

Figure 7. Waveforms Demonstrating Effects of Increasing n (Spacing)

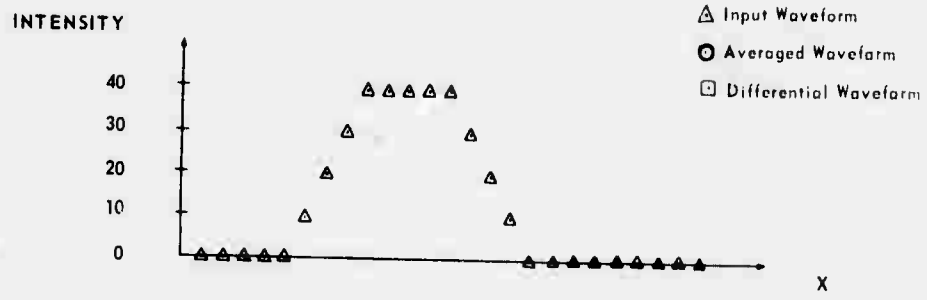

(a) Trapezoidal Input Waveform

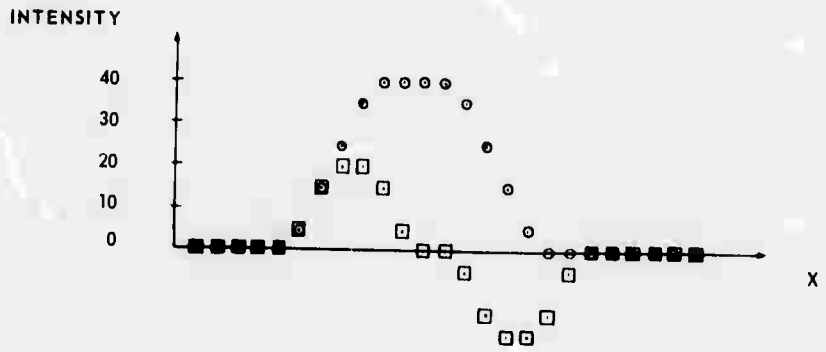

(b) Differential Waveform for mxn=2x2

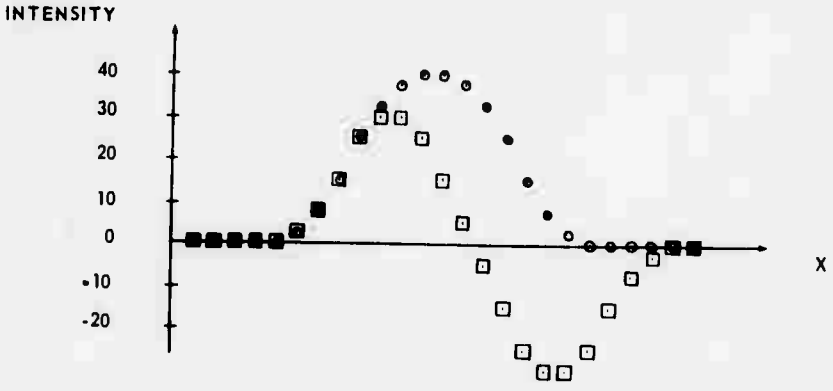

(c) Differential Waveform for mxn=4x4

Figure 8. Waveforms Demonstrating Advantages of Increased Spacing

(a) Averaging=1x1

(b) Averaging=4x1

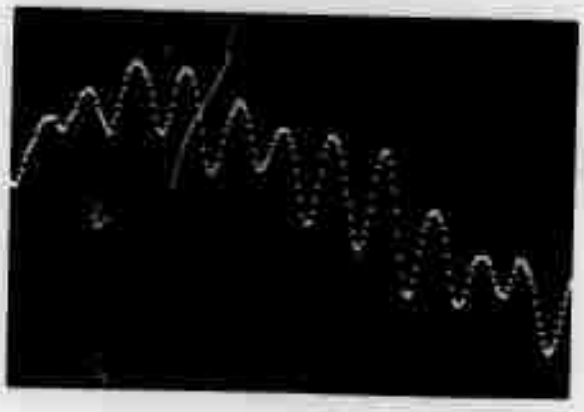

(c) Averaging=10x1

Figure 9. Intensity Profile for Micrometer Image Showing Effect of Increased Averaging

It is clear then that the error in slope is minimized by increasing both m and n. Further note that if the averages had been overlapping in such a way that the error point were included in both, then the error would have cancelled and would have not affected the approximation.

Another characteristic of this kind of averaging can also be seen in Figure 5. This characteristic concerns the relationship between m and the number of points on a part of the intensity curve with a certain slope. In particular, if m is greater than the number of points on the portion of the curve with slope K, then the maximum slope of the averaged curve will be less than K. Although this has the effect of attenuating the maximum slope of sharp edges, it is most effective in reducing the amplitude of noise because noise tends to be of short duration.

To provide further insight regarding the effects of m and n, a number of ideal input intensity sequences were made up and processed graphically. Figure 6 illustrates the results when m is increased while n remains constant (n = 1 for this series). The top trace illustrates the ideal input waveform as a function of distance, while the two below exhibit differential waveforms derived from the average signal for m = 2 and m = 4. Note that in the processed traces the effects of the edges are spread over a longer distance and that the amplitude of the signal is diminished.

Spacing effects are demonstrated in Figure 7. Again the input appears at the top and cases n = 2 and n = 4 are below (m = 1 for both cases). Observe that as before the effect of the edge extends further than in the input. Furthermore the signal amplitude, although again diminished, is not reduced as much as when m was increased proportionally in the previous figure. Hence increased spacing yields the significant benefit of increasing the output amplitude when it is employed along with greater points/average. This can be seen by comparing the 2-2 and 4-4 waveforms in Figure 8 with the 2-1 and 4-1 traces in Figure 6. For example, the differential waveform for 2-1 averaging in Figure 6(b) has a peak-to-peak amplitude of only 20_8, whereas the waveform in Figure 8(b), where 2-2 averaging is applied has a peak-to-peak amplitude of 40_8.

An example of an actual scanned line is seen in Figure 9(a). Notice the appearance of a number of small noise excursions from the main signal. In Figure 9(b) the same line has been preprocessed with parameters 4-1, and the waveform appears smoother, more continuous, and easier to interpret. Averaging with parameters of 8-1 has been applied in Figure 9(c), and the signal now appears even smoother. Observe, however, that the signal amplitudes have also begun to decrease, so that m cannot be raised much higher without making the significant intensity variations hard to detect.

3. OUTLINE TRANSFORMATION ROUTINES

Computer routines are developed which operate on the preprocessed intensity data with the goals of (a) displaying outlines corresponding to a selected range of input intensity transitions while (b) suppressing noise points and uninteresting small changes in signal level. Constraints imposed by the hardware also dictate certain features of these routines.

One method (later designated transformation SS) produces an edge point whenever the difference between adjacent preprocessed intensity points exceeds a threshold. The thick edges obtained in one mode of the program can be changed to a single point on each edge by switching to a more time-consuming thin edges mode. Transformation AC allows intensity differences to accumulate as long as they exceed one threshold and do not change sign, then compares the accumulated difference to a second threshold to determine whether or not an edge should be displayed. Some results of processing with the two procedures are given and their performance is compared.

3.1 INTRODUCTION

The specifications for a processor to detect and display object edges in an image for the general purpose measurement tool contemplated here include: (a) computation with sufficient speed to permit on-line performance, (b) display of two levels only, (c) edge detection during the line scan operation, (d) production of smooth outlines, (e) consistent edge location to promote easy correlation between display and measurement, (f) flexibility in selection of edges to be displayed. Speed and flexibility prove to be the most important attributes of the desired processors.

There are three main hardware constraints that also influence efforts to achieve suitable outline pictures. There are (a) slow instruction execution speed, which prohibits excessively long or difficult calculations, (b) small memory, which demands computations and decisions based on relatively small portions of the image, and (c) unavoidable noise from the image dissector, which makes necessary the use of some filtering technique. Other hardware limitations prove trivial by comparison with these three, and are therefore not considered here. These constraints, coupled with the specifications listed earlier, help determine the compromises discussed in the following paragraphs.

Since measurements of distance can only be made in one dimension at a time with a with a sequential machine, edge detection in one direction only is allowed by the specifications and one-dimensional processing is adopted to reduce the amount of memory required for data storage. This results in a less complicated, faster-running program which controls a simple raster scan. Processing in either direction (vertical, called the Y scan, or horizontal, called the X scan) may be obtained and after one-dimensional processing in both directions, horizontal as well as vertical edges are detected.

Because a two-level display suffices as an output device, the Tektronix 564 Storage Oscilloscope was used for that purpose. The 564 also adequately meets the specification of an on-line system because the operator can observe the display and interact with the equipment as an image is being produced. When the desired outline image has been developed, it can be saved on the storage scope while measurements or other operations are performed.

The specifications of speed and flexibility in developing outlines as well as the prohibition against time-consuming calculations lead to processing routines that are sequential

in a sense similar to the sequential operations defined by Rosenfeld and Pfaltz.[37] That is, the operations which determine where an edge is displayed in an output image are dependent not only on the input point presently being processed, but also on information from previously processed points. Rosenfeld and Pfaltz note that on a sequential computer this type of sequential processing is faster for many transformations than the corresponding parallel processing (where the new values at each point in the picture depend only upon the old input values and not on the previously processed values). However, the parallel processing performed on a parallel machine is faster than either of these. Thus, sequential operation and resistance to the effects of noise can be built into the transformations at the same time.

A good analogy by Roberts calls attention to the difficulty of the edge detection problem:

> A simple procedure might be to choose a clip level and start tracing outlines which correspond to a string of adjacent cells in the raster, all of whose [intensity] values are above the clip level. The hopelessness of this procedure is easily seen when one looks at typical pictures and considers them as a three-dimensional surface where the z [intensity] values are used as the height. Even a very clean input picture when viewed in this way looks like a bumpy, hilly landscape, with a broken-down stone wall replacing the lines, and where some hills are higher than the top of other stone walls. If we imagine the clip level as a flood over this landscape, there is no water level which covers all the hills and yet does not submerge some stone walls. In fact, even by adjusting the water level to be optimum for a particular area, a line will look like stepping stones in a rock-strewn brook rather than a smooth dam. Thus it can be seen that the problem of mapping the walls is not a simple one. [34, page 170]

Since the intensity data is rather difficult to work with as Roberts points out, the outlining transformations which follow are only steps in an evolutionary process. In this process a reasonable transformation is created after observing the input data. This transformation is tried on some typical images to see if it detects and reproduces the same edges seen by the human eye. Then the transformation is modified and refined if it is partially successful or discarded if it is not. The following processors are introduced in the order in which they were developed; the second one (AC) is considered more generally useful than the first (SS).

3.2 OUTLINING TRANSFORMATION SS

Abbreviations have been chosen to represent the two outlining techniques discussed here to simplify the abundant references made to them. These abbreviations are meant to be not so much precise acronyms as convenient ways to describe the techniques. Hence, the first transformation is called SS (for Steepest Slope) in spite of the fact that this acronym precisely names only one mode of the transformation. Similarly the second transformation is referred to as AC (for ACcumulation).

An appealing first attempt to solve the outline problem, which avoids the difficulties mentioned by Roberts, is to use an operation which effectively differentiates the input image. This is done in processor SS by comparing the absolute difference between adjacent preprocessed intensities to a threshold. A corresponding outline point is intensified on the output display only if the absolute difference exceeds the threshold. The threshold is adjusted by means of a LINC potentiometer input so that as the outline image is produced, the threshold may conveniently be raised to display fewer edges in a noisy picture or lowered to display more edges in a noise-free picture.

The operation just described constitutes what is called the thick edges mode of transformation SS. Although it processes an image very rapidly, the edges it displays are rather thick and hence for some cases the quality of the output image is not suitable for viewing or measuring. Furthermore, the threshold does not always provide the desired flexibility. For instance, actual object edges which one might wish to display may yield intensity differences smaller than those associated with noise points. Hence setting the threshold low enough to enable displaying the real edge points results in displaying the noise points as well. Consequently the output display includes a multitude of isolated noise points which camouflage and detract from the lines which represent the true outlines. An example of the output created by thick edges processing can be seen in Figure 11(a).

The thin edges mode of SS is designed to constrain the outline so that it is only one point thick. The method used to determine whether an edge point is displayed involves the assumption that the successive absolute differences between adjacent preprocessed intensity points are less than the threshold at least once between edges. Specifically, the edge point is not displayed even after the differences exceed the threshold until the greatest difference is encountered (hence, the acronym Steepest Slope). Then the point is displayed and the display routine is disabled until at least one absolute difference is less than the threshold. After the processor has located the maximum difference on an edge, several succeeding differences typically remain above the threshold and the processor remains disabled until a difference less than the threshold is encountered. If the SS processor receives a difference less than the threshold before the edge has been located, the point is displayed but the display routine is not disabled. Note that the signs of the differences are not considered; therefore, only one edge is detected and displayed if the intensity waveform suddenly changes slope as in Figure 10. However, this situation is highly unlikely in a physical environment because in general at least two points will have intensities near the maximum, thus creating a difference less than the threshold and causing an outline point to be displayed without disabling the display routine.

Perhaps the most concise way to describe the sequential action of the thin edges processor is with the state diagram shown in Figure 12. In state 1 the processor is enabled and the previous difference is less than the threshold; the program is started in this state at the beginning of each picture line. State 2 is a situation where the processor is still enabled, but the previous difference is greater than or equal to the threshold. The processor is disabled in state 3, which also corresponds to a condition where the previous difference is equal to or greater than the threshold. Notice that it is necessary to continually remember the previous difference when the processor is enabled, so that it may be compared to each new difference input to see if the maximum difference has occurred. Thus each new difference is compared first to the threshold and then to the previous difference.

Don't-care conditions also occur, due to certain physically impossible situations. For example, in state 1 the input combination X_1X_2 10 is a don't-care, because state 1 is defined by the existence of a previous difference less than the threshold, whereas the input specifies a present difference less than the previous difference but greater than the threshold. This is clearly impossible, so no transition labeled 10 leaves state 1. Similarly, no transitions from state 2 or 3 are initiated by the input combination X_1X_2 01.

The flow chart of Figure 13 shows how the state diagram described above is implemented. The thin edges transformation is entered at the top with a new computed difference (absolute value). Comparison of this present difference with the threshold, then the status of the display

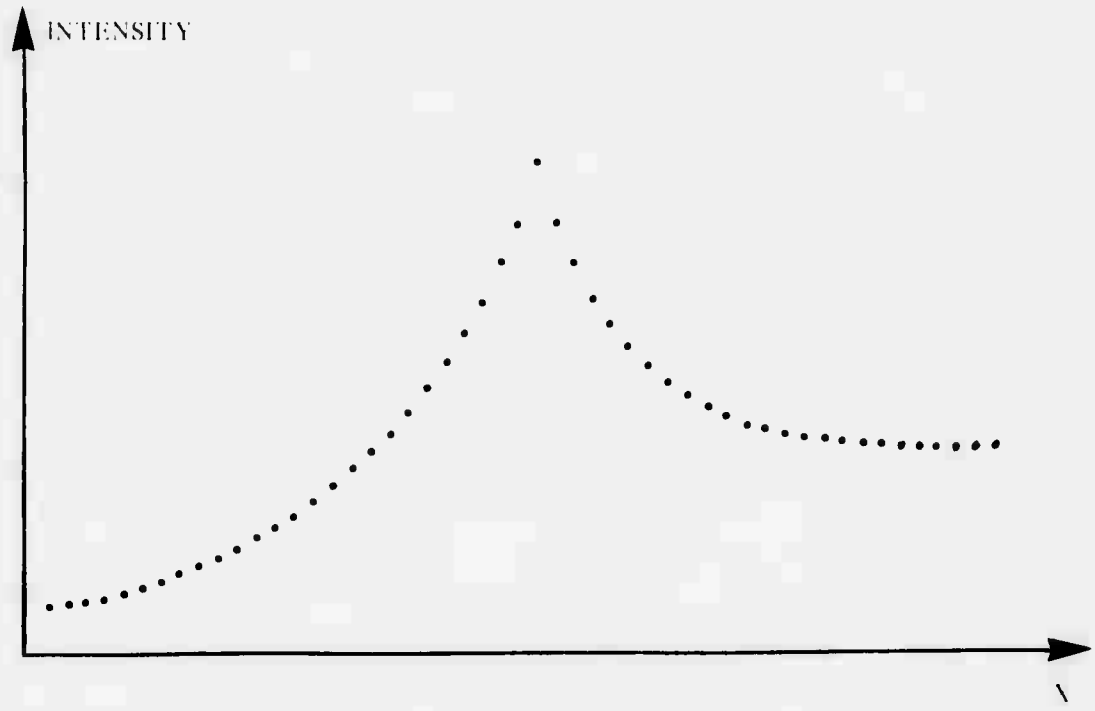

Figure 10. Intensity Profile Where Transformation SS Detects Only One Edge

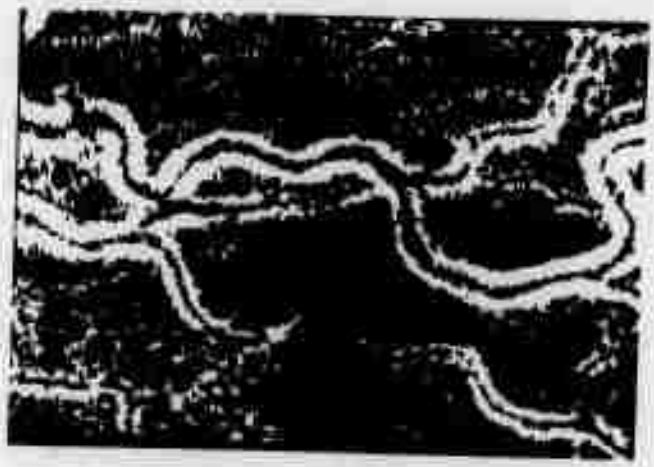

(a) Outlines of Rat Vessels Produced by Thick Edges Mode

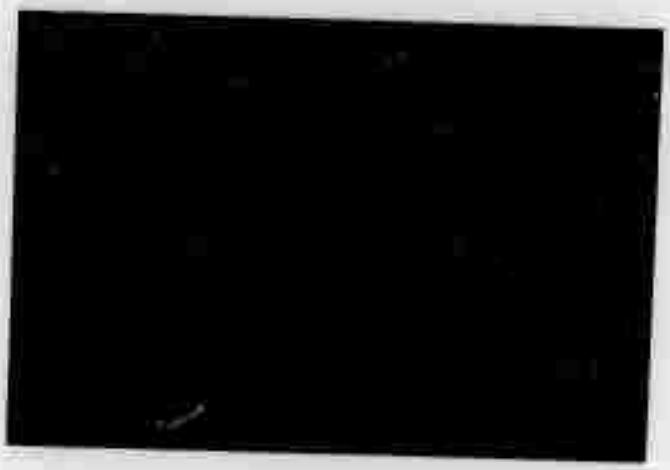

(b) Outlines of Rat Vessels Produced by Thin Edges Mode

Figure 11. Comparison of Thick Edges and Thin Edges Modes of Transformation SS

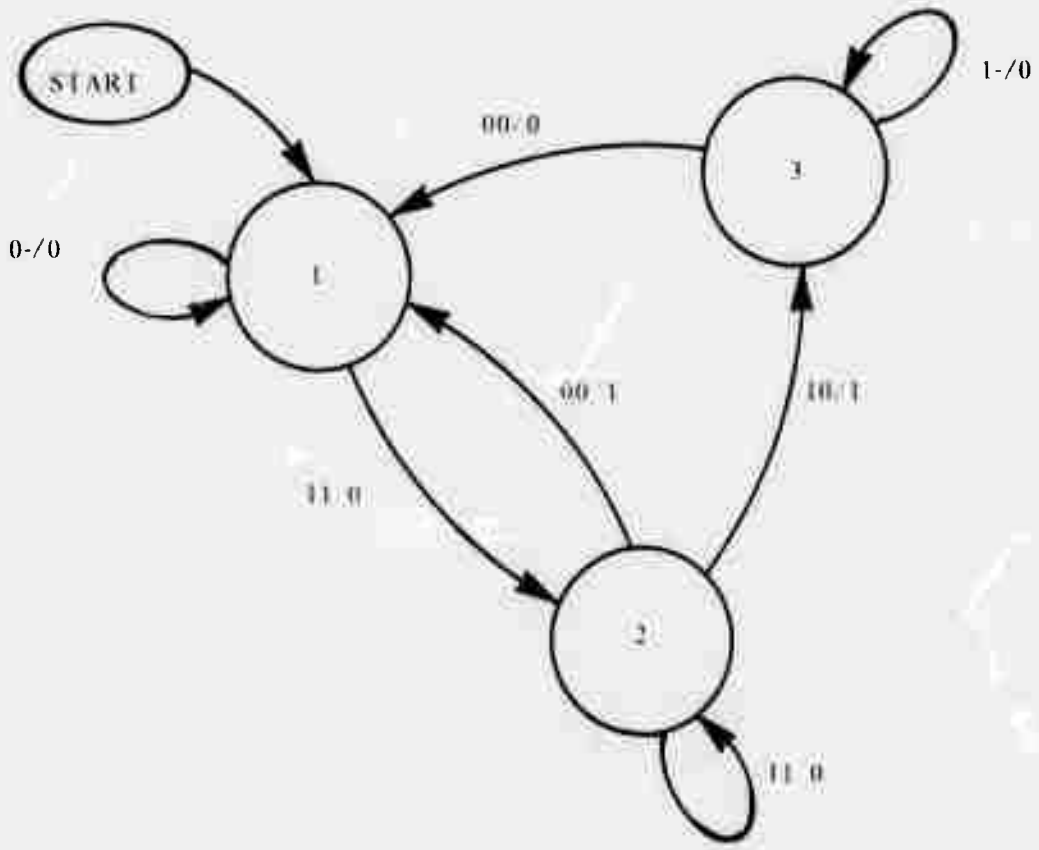

Transitions are labelled X_1X_2/Z, where

$X_1=0$ $\quad |\text{present difference}| < \text{threshold}$

$X_1=1$ $\quad |\text{present difference}| \geq \text{threshold}$

$X_2=0$ $\quad |\text{present difference}| \leq |\text{previous difference}|$

$X_2=1$ $\quad |\text{present difference}| > |\text{previous difference}|$

$Z=0$ no display

$Z=1$ display edge point corresponding to previous difference location

Figure 12. State Diagram for Transformation SS

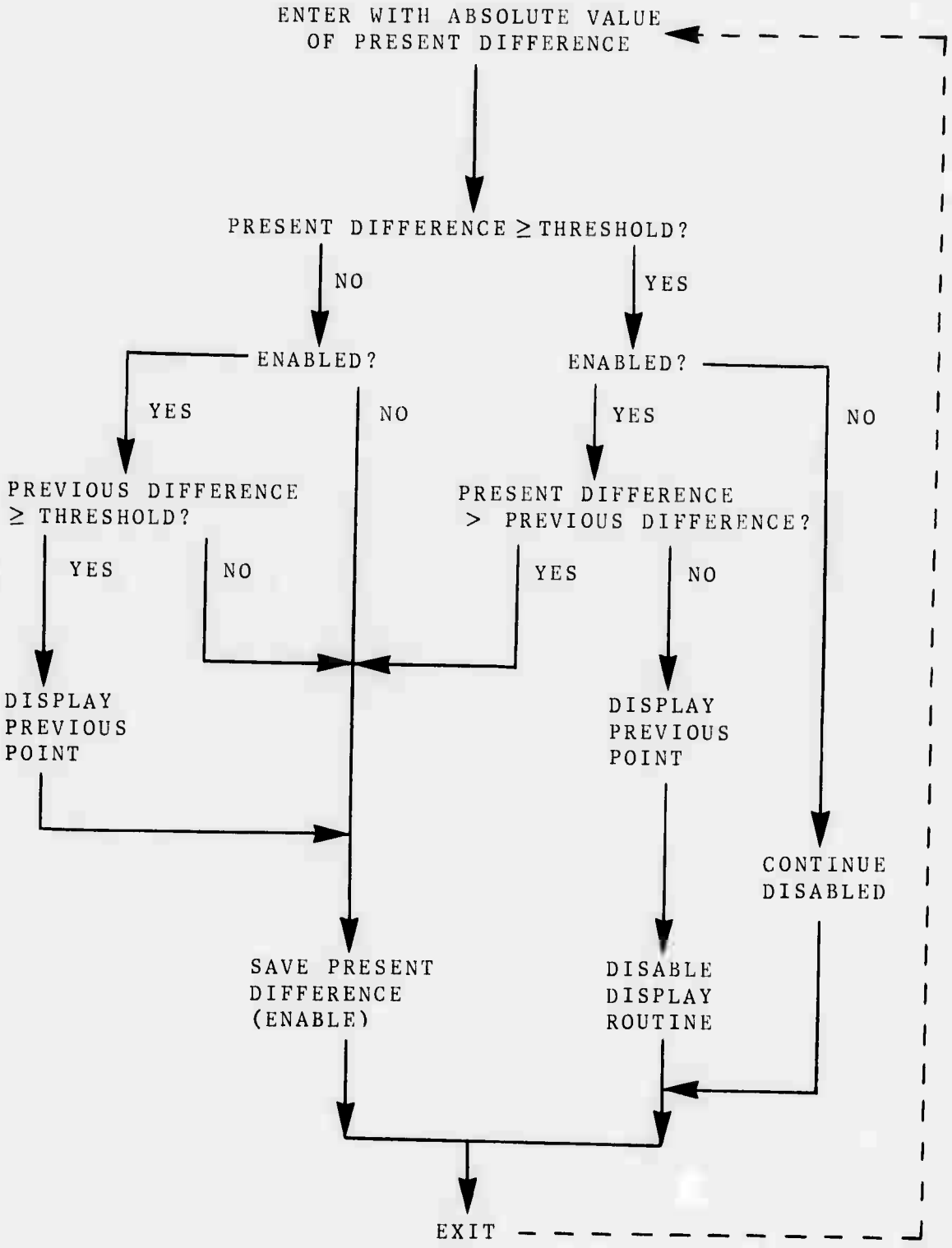

Figure 13. Flow Chart of Transformation SS

routine, and finally comparison of the present difference with the threshold or with the previous difference determine the final action. Note the dotted line which represents how the exit leads to calculation of the next difference and subsequently to re-entry into the routine (except at the end of a line, of course, when the scheme is reinitialized).

Although the thin edges processing takes about twenty-five percent more time than the thick edges mode, the resulting pictures are still obtained rapidly enough to allow good on-line performance. Moreover, the quality of the images is greatly improved by using the thin edges mode, as can be seen by comparing the (a) and (b) photographs in Figure 11. The actual location of the edge is much more distinct in (b), where thin edges processing was used, than in (a), which shows the application of thick edges processing to the same image. Furthermore, the amount of noise is significantly less in (b) than in (a), although the same threshold was in use for both pictures.

3.3 OUTLINING TRANSFORMATION AC

Experience with the first processor (SS) leads to consideration of other processors which are likely to supply better outlines and fewer noise points in the output image with greater flexibility. In particular the resolution of the edge detecting operation appears to be less than that of the whole system (due in part to the eccentricity described by Figure 10), and scanning a straight line develops an outline which has quantization notches due to the influence of noise. In addition, even in the thin edges mode the threshold is not sufficient to separate large noise pulses from small edge differences, although an observer can easily distinguish the two cases in waveforms which the computer analyzes. Hence, thought is centered upon aspects of the data which reveal intensity differences corresponding to object edges and which allow noise to be rejected by the system.

Two pieces of information essentially ignored by processor SS are immediately perceived as harboring potentially valuable hints regarding the existence of edges. These are (a) the signs of the differences between successive intensity values and (b) the magnitude of the sum of all the differences in a single transition. Specifically, intensity values at an object edge usually give rise to a sequence of differences whose signs are the same and whose sum is greater than the sum of differences where no edge exists. Therefore, intensity differences may be accumulated until their sign changes, and then the total accumulated difference may be compared with a threshold in order to decide whether the edge should be displayed. In this way the entire edge is used to decide whether to produce an outline point. Furthermore, by comparing the absolute value of each input difference with a second threshold, many differences can be ignored as too small to constitute part of an object outline. This follows from the observation that the slope of the intensity at a true edge is quite steep. Implementation of these ideas results in transformation AC. (The name derives from the fact that differences accumulate in this routine).

As described briefly above, AC uses two variable thresholds. Each preprocessed intensity difference is first compared to a relatively small threshold, which is called the noncumulative (NC) threshold because it is applied only to individual differences and not to accumulated differences. If the absolute value of the input difference is less than NC, no action taken and the next difference is calculated. If the input difference equals or exceeds NC, its sign is compared to the sign of the accumulated difference and when they are the same, the input is added to the accumulated difference. If the signs of the input and accumulated

differences are not the same, the accumulation is halted and the absolute value of the accumulated difference is compared to a second threshold. Because it is employed only in testing accumulated differences, this one is called the cumulative (C) threshold. If the accumulated difference is equal to or greater than C, a point is intensified on the output display to mark the edge detected. However, if the accumulated difference is less than C, no point is displayed because the edge is not considered high enough to be significant. Regardless of whether an outline point is displayed, a new accumulation begins whenever an input difference which exceeds NC has a sign different from that of the accumulated difference. It is also important to point out that during an accumulation, any difference input less than NC causes the accumulation to end. Again the accumulation is compared to C to determine whether the edge should be displayed, but in this case no new accumulation begins because the input does not indicate that an object edge exists.

Edges are placed by AC in the center of the domain in which accumulation takes place. That is, the scheme records the location where accumulating starts each time, and when accumulating stops, the last location is subtracted from the recorded first location to find the length of accumulation. If the accumulation exceeds C, the displayed point is in the middle of this accumulation interval. This philosophy works very well for symmetrical edges, but encounters some other problems as detailed in the next section.

Figure 14 is a state diagram which demonstrates the sequential action of transformation AC. State 1 is a nonaccumulating condition in which the processor continues as long as the differences are less than the noncumulative threshold. When NC is exceeded, the scheme enters state 2 in which differences accumulate until they change sign or again become less than NC. Note that the accumulated difference is compared to C (variable X_3) for these cases and that an edge point is displayed ($Z_1 = 1$) if C is exceeded.

The flow chart of Figure 15 may be an easier way to understand the state diagram just described. The first question (ACCUMULATING?) is implicit in the sequences which follow the comparison with NC and merely indicates the state of the program on the flow chart. START ACCUMULATING and STOP ACCUMULATING designate points in the process where the state of the program is changed. Either (a) a difference whose absolute value is less than NC or (b) one whose sign is different from the sign of the accumulation is sufficient to effect comparison of the accumulation with C, but only (a) causes accumulation to cease. Thus the resolution difficulty illustrated in Figure 10 is avoided because a sign change starts another accumulation after comparing the accumulation just finished to C. Although the flow chart shows the accumulation being reset after STOP ACCUMULATING when the previous accumulation is less than C, this reset value is used again only if the program continues in the accumulating state.

Photographs later in this work (especially in section 5.3) amply illustrate the quality of outlines produced by AC.

3.4 COMPARISON OF TRANSFORMATIONS SS AND AC

Since AC is the more recently developed transformation, it may seem reasonable to assume that it gives better results for all intensity waveforms. However, SS does retain some limited advantages, particularly regarding placement of edges. AC exhibits greater flexibility in general, supplying the ability to choose one of several ways to process the image whereas the first transformation forces a certain specified interpretation.

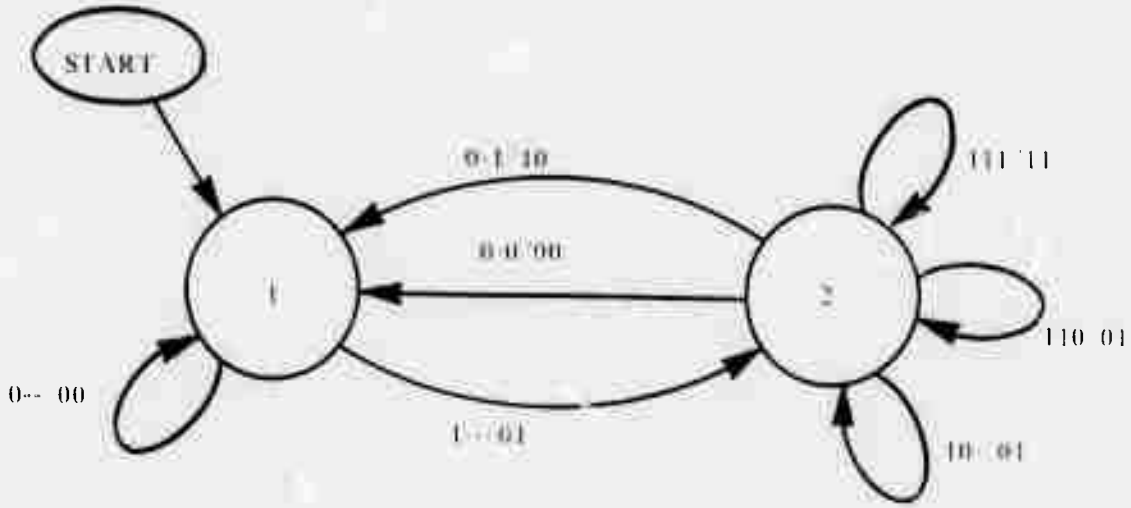

Transitions are labelled $X_1X_2X_3/Z_1Z_2$, where

$X_1=0$ |present difference| < NC

$X_1=1$ |present difference| ≥ NC

$X_2=0$ sign of present difference does not differ from sign of accumulation

$X_2=1$ sign of present difference differs from sign of accumulation

$X_3=0$ |accumulation| < C

$X_3=1$ |accumulation| ≥ C

$Z_1=0$ display no point

$Z_1=1$ display point corresponding to middle of edge sequence

$Z_2=0$ discard present difference

$Z_2=1$ add present difference to accumulation (start new accumulation if signs different)

Figure 14. State Diagram for Transformation AC

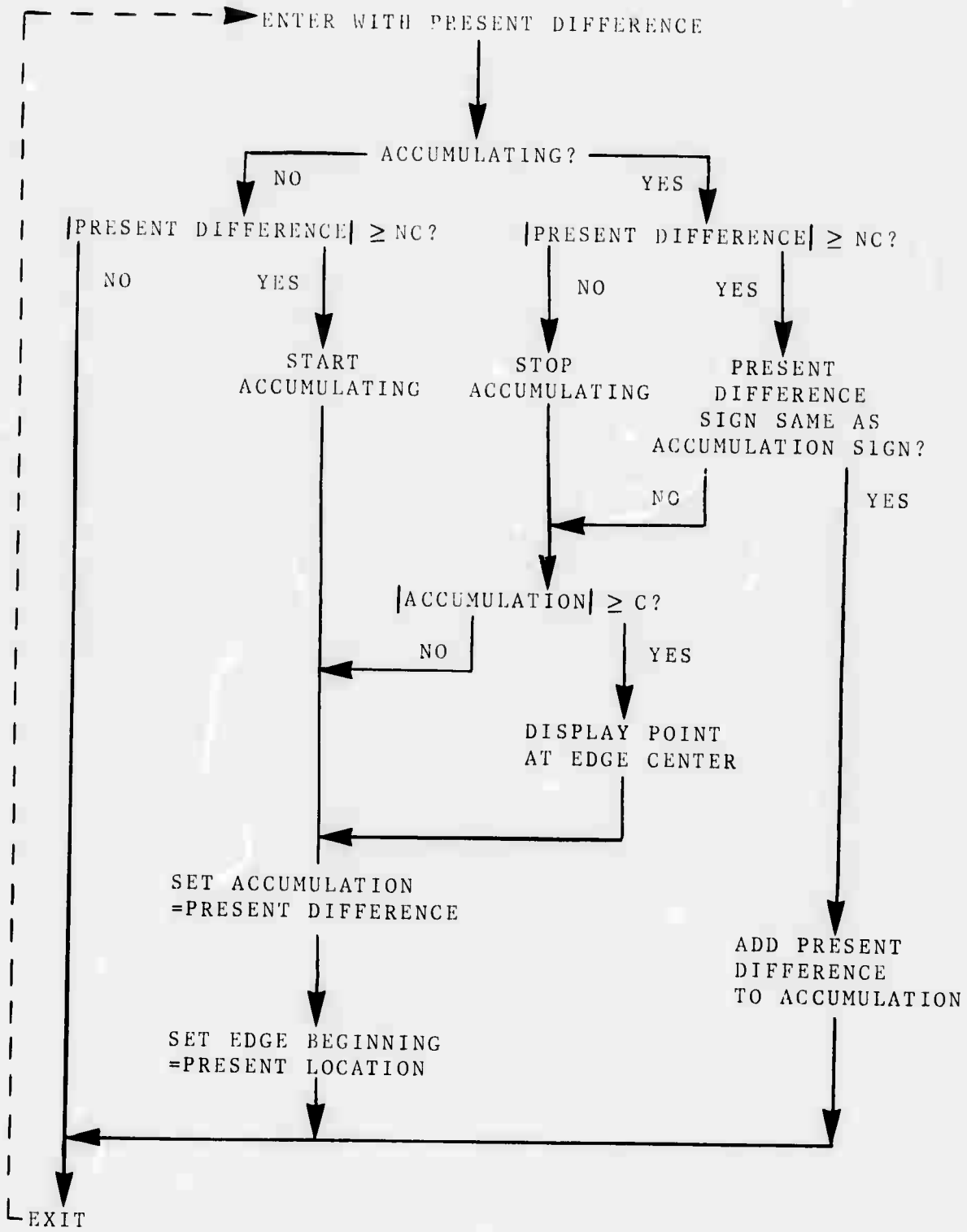

Figure 15. Flow Chart of Transformation AC

Allowing just one outline point to stand for a possibly long and complex transition of intensity introduces some interesting trade-offs in designing the processors. The first part of this section discusses the relative merits of the two procedures used for determining edge location. Next some photographs are presented to contrast the quality of output images created by the competing processors. Finally, an ideal intensity waveform is processed by both schemes and the results are compared.

Processor SS sometimes locates edge points better than AC does. For example Figure 16(a) shows an intensity profile for which the edge positions established by SS seem more reasonable that those specified by AC. Because the characteristic is steeper close to the peak between E and F, the points which represent the two sides of the peak should also be close to these locations. Transformation SS does in fact place the edge points at E and F. The other transformation, however, divides the accumulation intervals AE and EJ into halves and locates the intensified points at B $A+\frac{AE}{2}$ and I $E+\frac{EJ}{2}$. Even if NC is increased so that CE and EH are the accumulation intervals, transformation AC still does not give entirely satisfactory results. With NC high enough to place the edge dots at D $C+\frac{CE}{2}$ and G $E+\frac{EH}{2}$, the program may well eliminate entirely other edges which one might desire to display.

Although B, D, G, and I are indeed in the intervals AE and EJ which define the two intensity transition, E and F are better places to represent the transitions. This feeling is reinforced by Robert's observation that human capacity to detect an edge is a function of the square roots of the edge intensities [34, page 168]. Thus the steeper portion of an intensity transition should be easier to detect, and it follows that this portion is the more important region of the change in terms of its relative contribution to the total effect. Mach's work[22] agrees in a general way too, in that positions E and F are approximately the locations where the second derivative of intensity with respect to distance is greatest. Schreiber also offers photographs which demonstrate the insensitivity of the human eye to low spatial frequencies [38, pages 324-5]; hence, edge representations most accurately portray a transition when they are located close to its steepest slope.

On the other hand Figure 16(b) shows how transformation AC is sometimes superior to SS in terms of locating edges. Assuming that segments MO and TV have slopes (absolute value) less than NC, scheme AC locates edges at L $K+\frac{KM}{2}$, P $O+\frac{OQ}{2}$, S $R+\frac{RT}{2}$, and W $V+\frac{VX}{2}$. Even if MO and TV have slopes greater than NC, transformation AC puts edge dots at N $K+\frac{KQ}{2}$, and U $R+\frac{RX}{2}$, which are reasonable representations for the longer intervals KQ and RX. Observe the asymmetry introduced by transformation SS, however. Because this plan places an edge marker at the first point where the slope exceeds the threshold if the succeeding point does not manifest a greater slope, edges here are put at K, O, R, and V for a reasonable threshold. A slightly lower threshold allows edges at K and R only, thereby exaggerating the asymmetry even further.

Most actual waveforms encountered display simultaneously the changing slope effect in part (a) and the symmetry evident on both (a) and (b) parts of Figure 16. Therefore, the edge points are usually positioned at almost the same places by both processors. Nevertheless, some unusual waveforms produce different results depending upon the transformations used. Certain asymmetrical profiles are portrayed better by SS even though AC provides more flexibility. By contrast SS yields asymmetrical edge representations for constant slope waveforms.

Figure 17 illustrates the line straightening effects of AC. Specifically, Figure 17(a) shows the outlines made by SS: these lines have obvious notches and irregularities. In contrast the lines created by the other transformation, shown in Figure 17(b), are relatively straight. This improvement is primarily due to the introduction of NC in this second scheme which only considers the rather large intensity differences associated with the steepest part of edge variations. When only a single threshold is used, as in the first transformation, quite small changes in the intensity signal are enough to cause slight shifts in the edge location from one line to the next. These small shifts combine to generate the notched effect in part (a) of the figure.

Resolution is improved by using the second processor, as also demonstrated in Figure 17. Processor SS misses some of the lines associated with the smallest bars (on the right side), but AC consistently fills in both edges of these bars. The assumption that there exists at least a short plateau between any two consecutive edges is to blame for the lack of resolution displayed by SS. As can be seen in Figure 17(c), no such plateau exists in this waveform: the crest is merely a single point, which certainly violates the assumption. Transformation AC, as was explained earlier, contains no such flaw and starts a new accumulation as soon as the difference signs change.

An ideal intensity profile, shown in Figure 18(a), demonstrates the location of outline points by processors SS and AC. The original graph of intensity versus distance consists of three sets of paired peaks superimposed on a slope of one. Each set contains on the left a peak whose amplitude is about 100_8 and on the right a peak whose amplitude is about 40_8; before being superimposed on slope one, the absolute values of the slopes of the three sets of peaks were 2, 3, and 4 in order from left to right.

Programs which apply transformations SS and AC to a line of intensities stored in the LINC produced the series of line segments seen below the input sequence in Figure 18. These programs display the detected outlines repeatedly line after line in order to facilitate studies of edge location.

In particular, Figure 18(b) illustrates the thin edges mode of processor SS. The series of five sets of lines corresponds to (from top to bottom) thresholds of 5, 4, 3, 2, and 1. Observe that as the threshold is decreased, more and more edges appear. This is a consequence of the admission of lower and lower slopes by the threshold. Also note that the outlines generated by SS appear directly below the changes in slope in the intensity profile. Placing the outlines in this way results from the fact that the profile possesses constant slopes,so that the first difference on each edge is also the greatest difference.

Figure 18(c) and (d) were generated by AC from the same intensity sequence in Figure 18(a). In part (c) the NC threshold is lowered from top to bottom, using the same values (5, 4, 3, 2, and 1) as in Figure 18(b) and with about the same results in terms of edges detected. However, the obvious difference in comparing the AC outlines with the SS outlines is the location of the edges. As discussed earlier, the outlines produced by AC are located in the center of the detected edge.

As the C threshold is gradually lowered in Figure 18(d) from the top to the bottom of the picture, more and more outlines appear. It will be recalled that the total amplitude of the detected edge is compared to C to determine whether to display the corresponding outline. Hence, the longest edges are present even at the highest C. Observe that the outlines selected with C are different from those selected with NC: this fact constitutes part of the power of transformation AC as compared to SS.

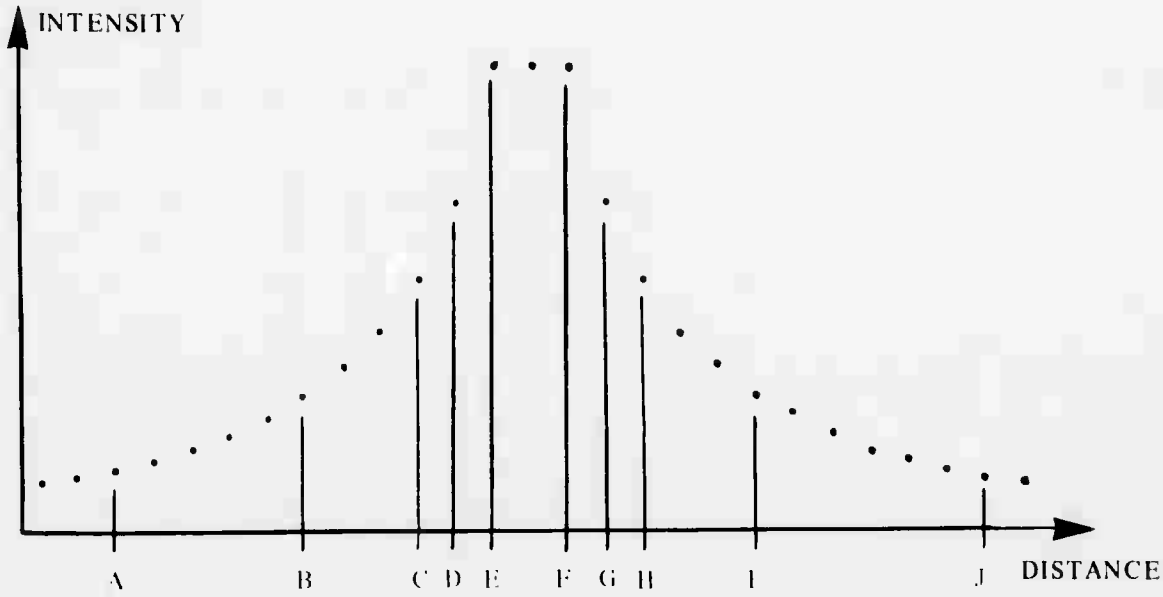

(a) Profile Showing the Advantage of Transformation SS

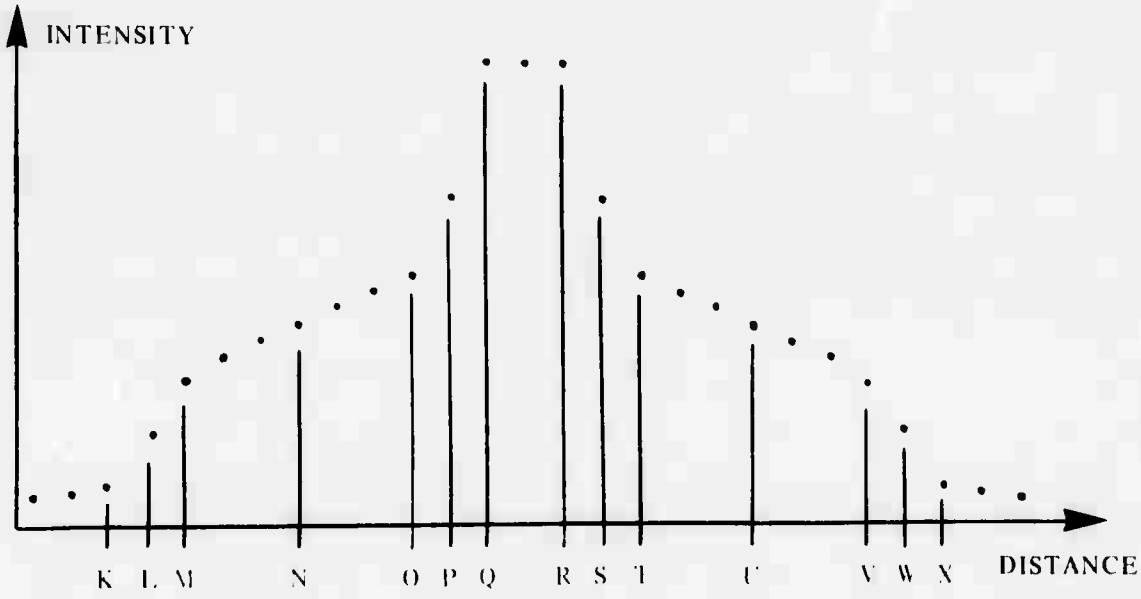

(b) Profile Showing the Advantage of Transformation AC

Figure 16. Intensity Profiles for Comparison of Transformations SS and AC

(a) Outlines of Bars Produced by Transformation SS

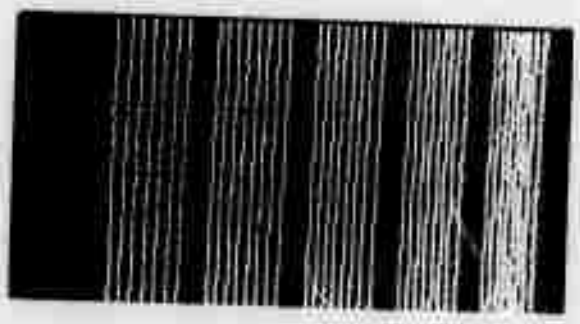

(b) Outlines of Bars Produced by Transformation AC

(c) Intensity Profile of Bars

Figure 17. Comparison of Bar Outlines Produced by Transformations SS and AC

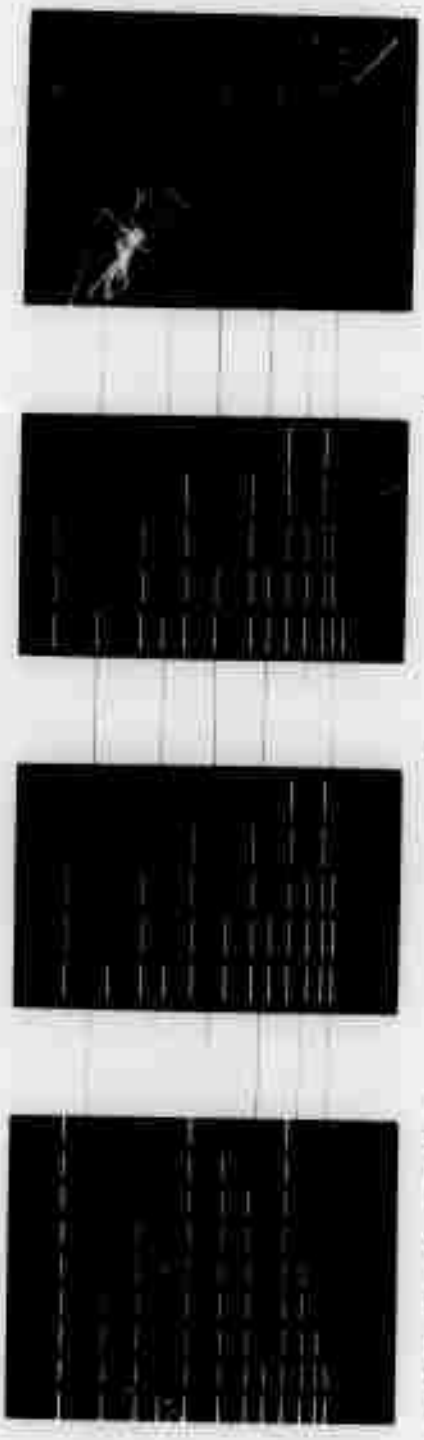

(a) Ideal Intensity Profile

(b) Transformation SS (Changing Thresholds)

(c) Transformation AC (Changing NC, C=0)

(d) Transformation AC (Changing C, NC=1)

Figure 18. Influence of Thresholds on Outlines Produced by Transformations SS and AC

4. AUXILIARY ROUTINES

Used in connection with programs which implement the outline transformations described in the last chapter, various subsidiary routines give the operator better means of monitoring the system and better methods of controlling it. One routine permits selection of the size and location of the scanned area. On command, another routine displays the intensities being scanned, either as a function of distance for a particular line or in the form of a histogram for an entire image. Contrast enhancement can be used to amplify certain intensity ranges chosen with the aid of the histogram.

Miscellaneous routines include a section for calibrating the measurements and a section for indicating the measurement segment. Another miscellaneous routine prints on the teletype values of program parameters in use at a particular time.

Another important set of routines controls measurements made by the system. Periodic automatic measurements can be made with any desired time delay between them,or a measurement can be initiated by the operator from the LINC keyboard at any time. Individual measurements can be repeated a number of times and added to provide a time average. Space averages, in conjunction with time averages if desired, are obtained by an averaging individual measurements along regularly spaced lines parallel to the measurement segments initially specified. Measured distances after averaging are automatically printed on a teletype connected to the LINC.

4.1 SCAN MANIPULATION

Programming convenience dictates a decision to make the size of the primary field of view no greater than one quadrant of the image dissector camera's field of view. However, some images require greater resolution than that afforded by this size. Occasionally the field of view is subject to motion (See section 5.3 for a brief discussion of the problems inherent in viewing biological specimens under magnification.); it is then imperative to complete the outline image as swiftly as possible. Because there is no immediate way to see the portion of the image being processed by the system,a means of mapping the camera field was developed.

4.1.1 ENLARGEMENT AND REDUCTION

By choosing one quadrant of the current field of view and dividing the digital increment between sampled points by two, a unique enlarged display of one sixteenth of the camera field can be developed. In fact, the system has the added ability of enlarging a second time to display one sixty-fourth of the camera field. Moreover, by storing the quadrant numbers chosen, the program can reduce the display to the previous one sixteenth or one fourth camera field upon command. In each of the above views, the display covers the entire face of the oscilloscope.

Reducing the time to produce an outline image is accomplished by dividing the number of sampled points by four. Resulting pictures cover one fourth of the screen. This "fast-window" process can be repeated until the display is very fast and very small, yet large enough to permit inspection of the salient image features. Of course a corresponding "slow-window" routine enables the display to be enlarged step by step until it covers the entire oscilloscope screen. Each time the size of the display is reduced, its location on the oscilloscope screen is assigned according to the quadrant numbers most recently specified in the

enlargement routine described above. When, for example, the interesting features in the original display appear in quadrant three, the third quadrant can be enlarged to cover the entire display. If more speed is necessary without greater resolution the command "fast-window" now yields a third-quadrant display only in one fourth the time.

A full-sized display of an outline image is seen in Figure 19(a), while Figure 19(b) shows an enlargement of the second quadrant of the same picture. (See picture credit, page 54.) Notice that more detail can be seen in the second picture, as expected when greater resolution is made possible by dividing the scan increment in half. An example of the "fast-window" for this enlargement appears in Figure 19(c). Notice that this display occurs in the second quadrant because the second quadrant has previously been enlarged.

A final aspect of scan manipulation is the raster sequence. While it might seem that other conventions would be required to correct for optical inversions, in fact it is possible to always scan points left to right within a line and lines top to bottom within a picture. Switches in the LINC digital-to-analog converters which control X and Y deflections on the displays allow reversals of the displayed image, right to left and/or top to bottom. Since a variable number of inversions of the image are introduced by the mirrors and lenses in the optical system, it is particularly advantageous to be able to correct new inversions by changing switches. To make the image appear in its natural or most convenient orientation, it would otherwise be necessary to include program routines to reverse the scan or display directions.

4.1.2 CAMERA FIELD MAP

Previously when the image processing system was used strictly for scanning transparencies, the following method was provided for determining which portion of the transparency would be scanned: the computer was put into a loop in which the intensity of a starting location previously selected with the LINC potentiometers was continuously sampled. Then by observing the deflection of a meter monitoring the intensity voltage input to the LINC while simultaneously moving some obstruction across the face of the panel fluorescent light source to interrupt the light to the camera, this location could be pinpointed. However, it was difficult to gauge the position and extent of the total area to be scanned by this method, or even to ensure that this area was entirely inside the camera's field. (Starting locations near the boundary could result in placing part of the scan outside the field.) Using a microscope image input compounds the difficulty because there is no easy way to see exactly where the light is interrupted in an image.

Therefore a map was devised which consists of a small square whose border represents the boundaries of the camera field. Displayed in the upper right corner of the output oscilloscope when in use, this map contains four points which mark the corners of the scan in progress when the map display was initiated. These points reflect the size of the scan field by their separation from each other and the location of the scan field in the camera field by their relation to the borders. Potentiometers on the LINC allow moving the dots within the border, thus also moving the scan area within the camera field. This facilitates searching for the most desirable expanse to be scanned and ensures remaining inside the camera's field by limiting the dots to move only within the map boundary.

4.2 INTENSITY MONITORING

Intensity histograms or spectrums are often used in image processing for monitoring the input intensities.[4,21] Although a histogram is often useful for evaluating the input intensities

(a) Original View of Four Quadrants

(b) Enlargement of Quadrant Two

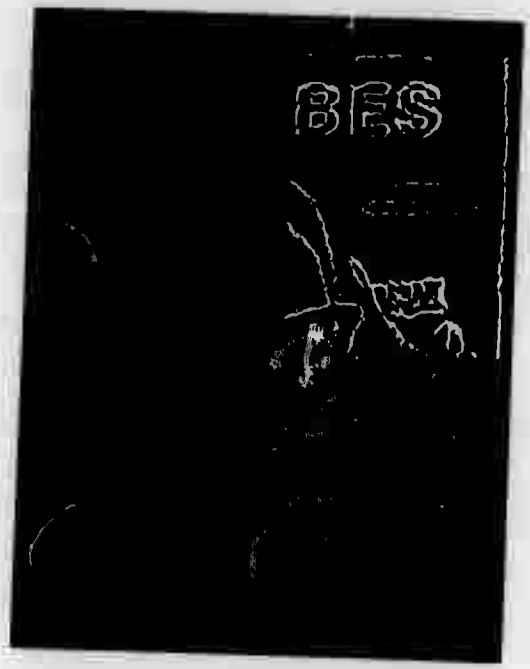

(c) Fast Window View of Quadrant Two

Figure 19. Enlargement and Fast Window

averaged over an entire image, the intensity profile of a single line lends assistance in attempts to understand specific details in the picture. Contrast enhancement, a digital means of increasing contrast in an image, is used in preprocessing when necessary.

4.2.1 INTENSITY LINE DISPLAY AND HISTOGRAM

The intensity line display (also called a single trace) merely plots a line of sampled digital intensities versus distance along the scanned line. This display is automatically turned 90 degrees when the scan direction changes. Thus the X scan intensity increases from the bottom of the scope to the top and distance in the image runs from left to right. In the Y scan intensity increases from the right to the left and distance in the image runs from bottom to top. These orientations permit easy comparison of outline points with the particular intensity variations that produced them. In addition, changing a LINC sense switch enables the operator to see the line after averaging instead of the raw sampled intensities. Appropriate scaling and translation can also be accomplished with the program to conveniently display the resulting plot.

Another useful feature of the intensity line display is its ability to lock onto a certain line on command and repeatedly scan it. By carefully observing the intensity trace of a single typical line, it is possible to estimate values of m, NC, and C which will improve the appearance of the outlines. Moreover, the intensity line display often proves invaluable for adjusting the preprocessing amplifiers when a microscopic image is being scanned, since the effects of both offset and gain are easily examined in this mode.

Figure 20 demonstrates the intensity line display. (By studying this intensity profile a better understanding of Robert's comments in section 3.1 can also be gained, for it is obvious that no single level can be set which will detect all the edges in this line.) The single trace at the top is a plot of the intensity samples from the line which is intensified in the outline image below. Note that outlines are produced (in lines adjacent to the intensified marker) at points which correspond to rapid transitions in the intensity profile above.

As intensities are sampled by the camera, a histogram is constructed which can be displayed on command. This display plots the number of points at each intensity versus intensity. Adjustment of preprocessing amplifiers and selection of appropriate parameters for contrast enhancement (described in section 4.2.3) are two uses of this histogram. See Guignon and Kline [21, pages 44 and 46-8] for further details. An example of this display can be seen in Figure 21. Intensity increases from left to right and the number of points increases from bottom to top. The diamond-shaped set of points together with the vertical line of points above it is a pointer, used to determine the parameters required for contrast enhancement.

4.2.2 CONTRAST ENHANCEMENT

By multiplying input intensities by appropriate factors (called slopes), the output contrast between any given point and its surrounding points (background) can be increased (enhanced) if the factor is greater than unity, or decreased (compressed) if the factor is less than unity. Care must be taken not to exceed the intensity range of the output device in using enhancement, but many images are considerably improved when such processing is applied. The singularly concise scheme for implementing this method has been fully described by Guignon and Kline [21, Chapter 4]

Figure 20. Intensity Line Display for Typical Line of Fly's Wing Image

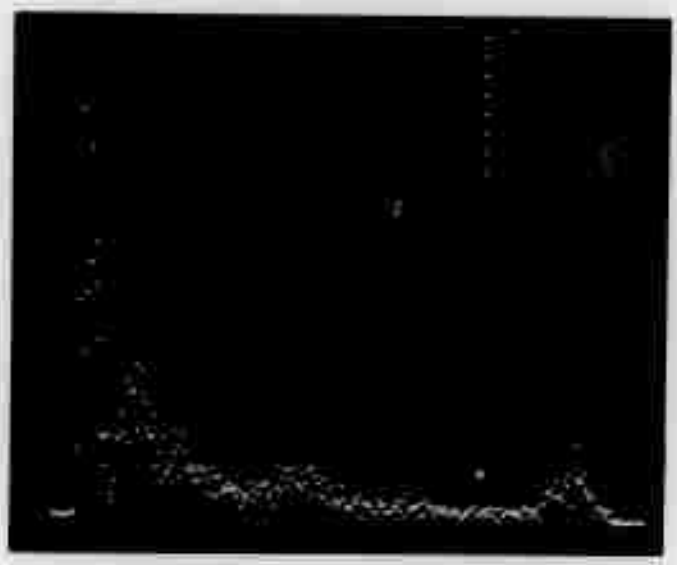

Figure 21. Typical Intensity Histogram

4.3 MISCELLANEOUS

Certain secondary routines that do not fit into the other classifications in this chapter are now explained. Some aspects described here will be needed in the next section which describes measurements.

Approximately thirty-five important parameters are used to describe and control the system performance. Some of these are altered infrequently by the operator to allow some special processing (e.g.: number of points averaged in the preprocessor) while others are changed on-line (e.g., coordinates of the area being scanned). A routine is included for printing upon request a teletype copy of the current parameters to provide a permanent record of the system's total state or an immediate diagnosis of system difficulties. Calibration parameters are stored by a routine which thus provides a means of specifying the scale to be used in measurements. Similar methods are used to precisely designate the so-called measurement segment between which the measurement routine searches for edges. Finally, there is a method for producing a halftone picture of the same area that is being outlined.

4.3.1 CALIBRATION AND MEASUREMENT SEGMENT INDICATOR

Calibration of the measurements is achieved by indicating some known length from the display and then typing this length on the LINC keyboard. A stage micrometer is placed in the microscope field to furnish a known length and an outline image of its scale is produced on the display by the same methods used to outline blood vessels and other objects. (Figure 22 shows a stage micrometer outline image.) When the stored image has been completed, the program is placed in the calibration mode in which a non-storing pointer appears superimposed on the image. By means of the LINC potentiometers this pointer is located on some line in the image; then by pressing an appropriate LINC key, the pointer position is marked on the display and at the same time its location is saved. By moving the pointer to another line and again marking its position as well as saving it in the computer memory, the desired distance in terms of display coordinates is indicated. The calibration length indicated by the dots in Figure 22 (marked with a C) is 100 microns. After the distance in microns between the dots has been typed into the computer, the program calculates a calibration ratio of microns to display distance. Thereafter, measurements are calculated in display distances and are multiplied by the calibration ratio to yield corresponding micron distances which are printed out.

To indicate where to measure in an image, the pointer subroutine that is used in the calibration routine is called again. As described above, a pair of endpoints are selected by the operator using the LINC keyboard and potentiometers. These endpoints are also marked on the display. (Two such pairs of measurement endpoints, both marked with an M, can be seen in Figure 22.) The display coordinates of these endpoints are converted to corresponding scan coordinates and stored as parameters for use by the measurement routine, which is described in section 4.4.

4.3.2 PARAMETER PRINTER

As explained briefly in the introduction to section 4.3, a parameter list controls the performance of the system. Examining this list often provides help in debugging additions to the programs, since all routines communicate with this list. Moreover, a printed record of the list facilitates labeling photographs produced by the system. Hence, a routine is included to

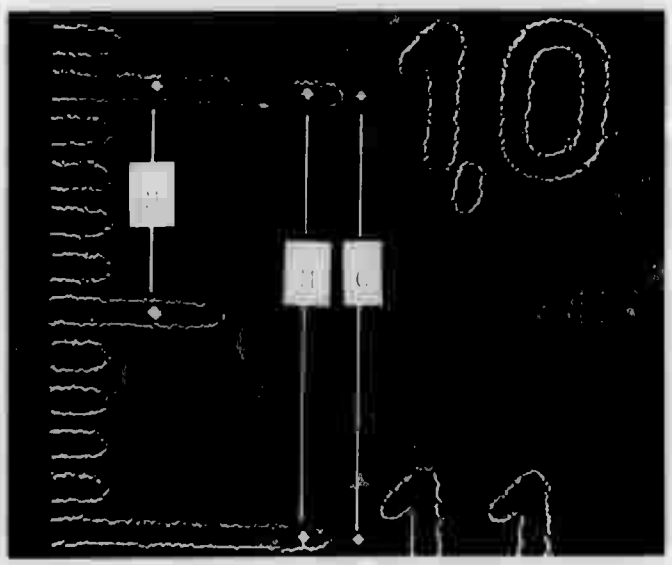

Figure 22. Stage Micrometer Outlines, with Measurement and Calibration Indicators

type out the parameters on a teletype connected to the LINC. In a long version the entire parameter list is printed with accompanying identifiers whereas a shorter option prints only the most important variables in a pre-arranged format without identifiers. Examples of both forms may be seen in Figure 23. In the long form many of the parameters can be recognized by the reader, including m (PT/AVE), n (SPACING), and the non-cumulative threshold (NC). In the shorter version the first line has the format m × n, the second line has the format NC C, and the remaining lines are contrast enhancement information.

4.3.3 GRAY LEVEL IMAGE

Since outlines of objects are sometimes ambiguous or hard to understand if one is not familiar with the objects as they appear in the field of view, it is helpful to have a picture of this field of view with several levels of gray. Therefore, a routine is provided to produce a halftone picture of exactly the same area for which outlines are being generated. An intensity step wedge can also be requested in order to calibrate the intensity of the Tektronix 561 output display. Various photographs in this work, including Figure 28(a) and 30, were made by means of the gray level routine.

4.4 MEASUREMENT

A general flow chart of the measurement routine may be seen in Figure 24. After the measurement segment has been indicated, the measurement operation itself may be initiated at any time from the keyboard. Another mode is also available which will initiate measurements periodically with precise computer-controlled intervals of delay between them. Thus, the measurements can be made fully automatically after the desired measurement segment has been specified. A number of sequential measurements may be averaged together to form either a space average or a time average, as explained below.

A portion of the program called the MEASURE subroutine forms the foundation of single, time averaged, and space averaged measurements. Its flow chart, seen in Figure 25, reveals that it begins very much like the outline program by sampling intensities on the measurement segment and processing them to detect edges. The sampling, preprocessing, and transformation operations are under the control of the same parameters that regulated the outline generation. Therefore measurement processing should detect the same edges as were detected by the outline processing, and these are again intensified in the display to give a visual indication of any translation or size change in the measured object. Moreover, the locations of the edges encountered are saved and the number of edges detected is counted. If the number of edges is exactly two, the distance between them is calculated from their locations, and this distance, after being multiplied by the calibration ratio, is ready to be printed on the teletype as shown at the bottom of Figure 24. Returning to Figure 25, one sees that error signals are printed if fewer or more than two edges are detected; when these signals occur too often, it is clear that the parameters of the system are not well-adjusted and they can then be optimized.

Figure 26, a flow chart of the TIME AVERAGE subroutine, helps explain how that part of the program averages a number of measurements to obtain a more accurate final value. Basically this subroutine merely calls the previously dsecribed MEASURE subroutine a number of times which is specified in the parameter list and monitors the measurements obtained. If exactly two edges are detected in the MEASURE subroutine, then the length obtained is added

```
07-22-68,15.55
4A 0001 PT/AVE
4B 0001 SPACING
4C 0377 X PT/LINE
4D 0377 Y PT/LINE
4E 0003 C
4F 0000 DISPLAY L
4G-0377 DISPLAY R
4H 0002 DISPLAY INCR
4I-0004 SCAN INCR
4J-0524 SCAN L
4K-0044 SCAN T
4L-2520 SCAN R
4M-2040 SCAN B
4N-0010 HISTO LINE INCR
4O 0001 INTGR CAL MULT
4P.6222 FRAC  CAL MULT
4Q 0001 MAX END PAIRS
4R 0001 END PAIRS
4S 0004 NC

 0000  0000
 0001  0001 BP1
 0002  0002 BP2
 0377  0377 BP3
 0400  0400 BP4

 0001 .0000 SLOPES
 0001 .0000
 0001 .0000
 0001 .0000

9A-1170 XL1
9B-0500 YT1
9C-1170 XR1
9D-1514 YB1

4T 0004 SM
4U 0004 TM
4V 0004 SZ+TZ
```

(a) Long Form

```
07-22-68,16.00
 0001 X 0001
 0004   0003
 0001 .0000     0001
 0001 .0000     0002
 0001 .0000     0377
 0001 .0000     0400
```

(b) Short Form

Figure 23. Parameter Lists Printed by Program on Teletype

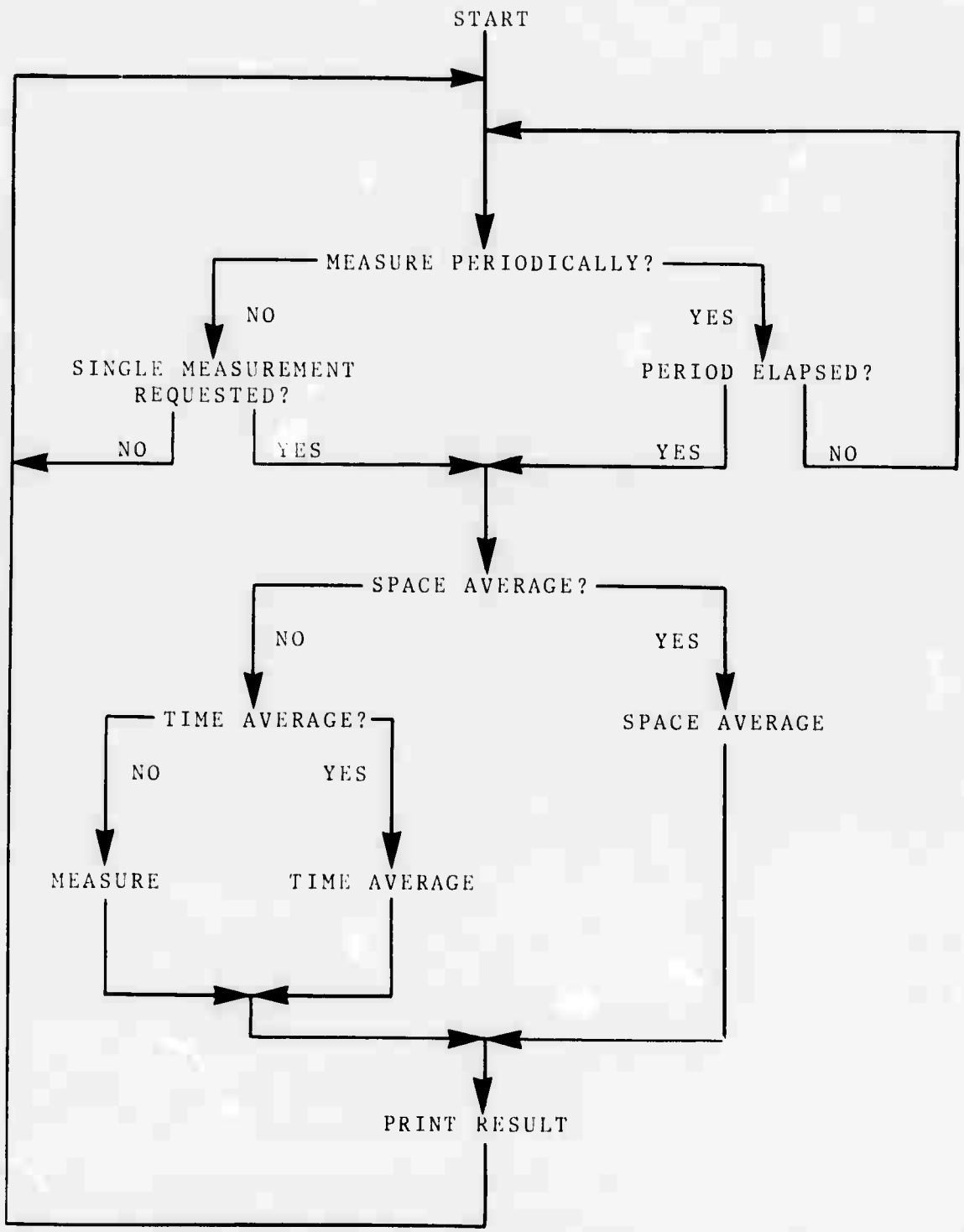

Figure 24. Flow Chart of Measurement Routine

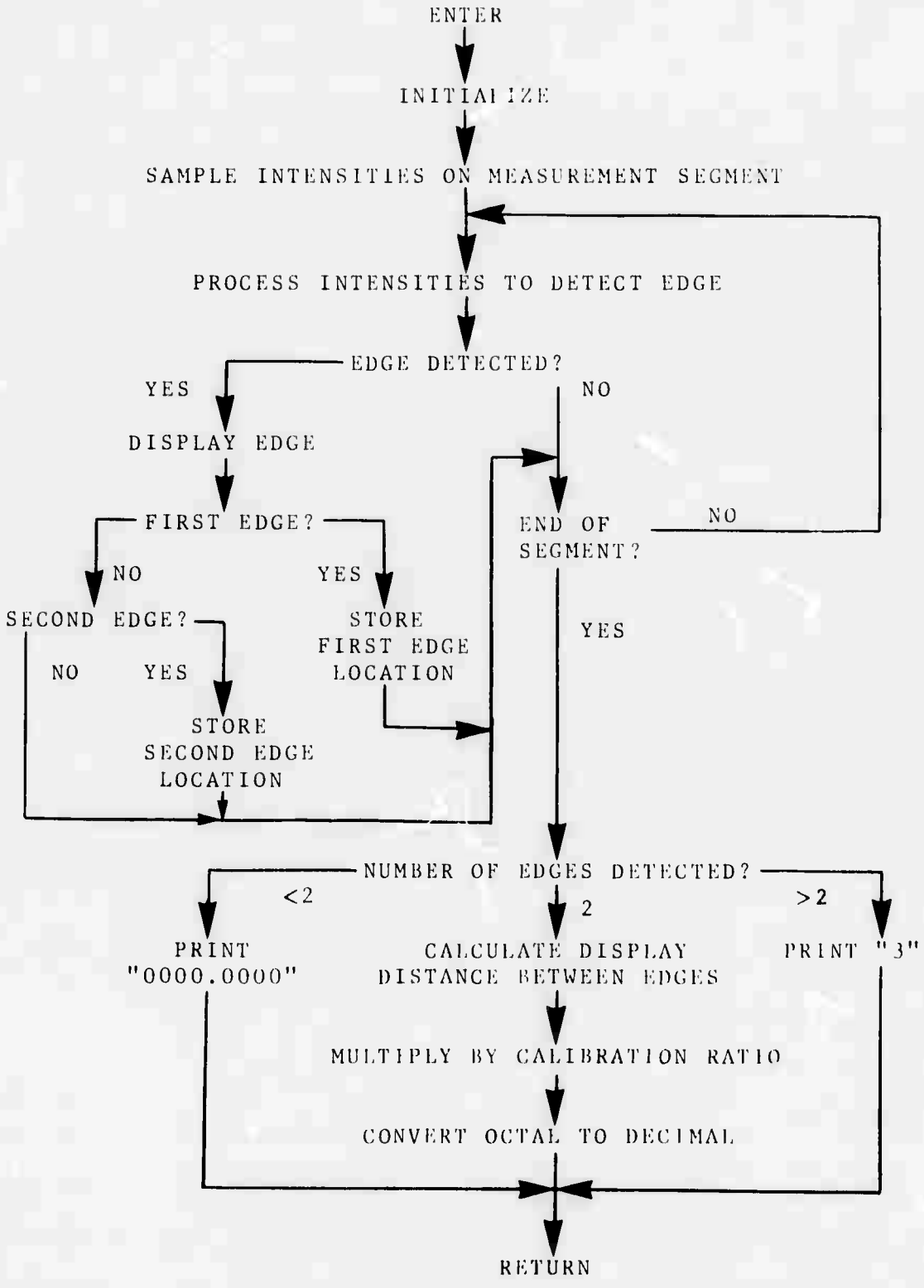

Figure 25. Flow Chart of MEASURE Subroutine

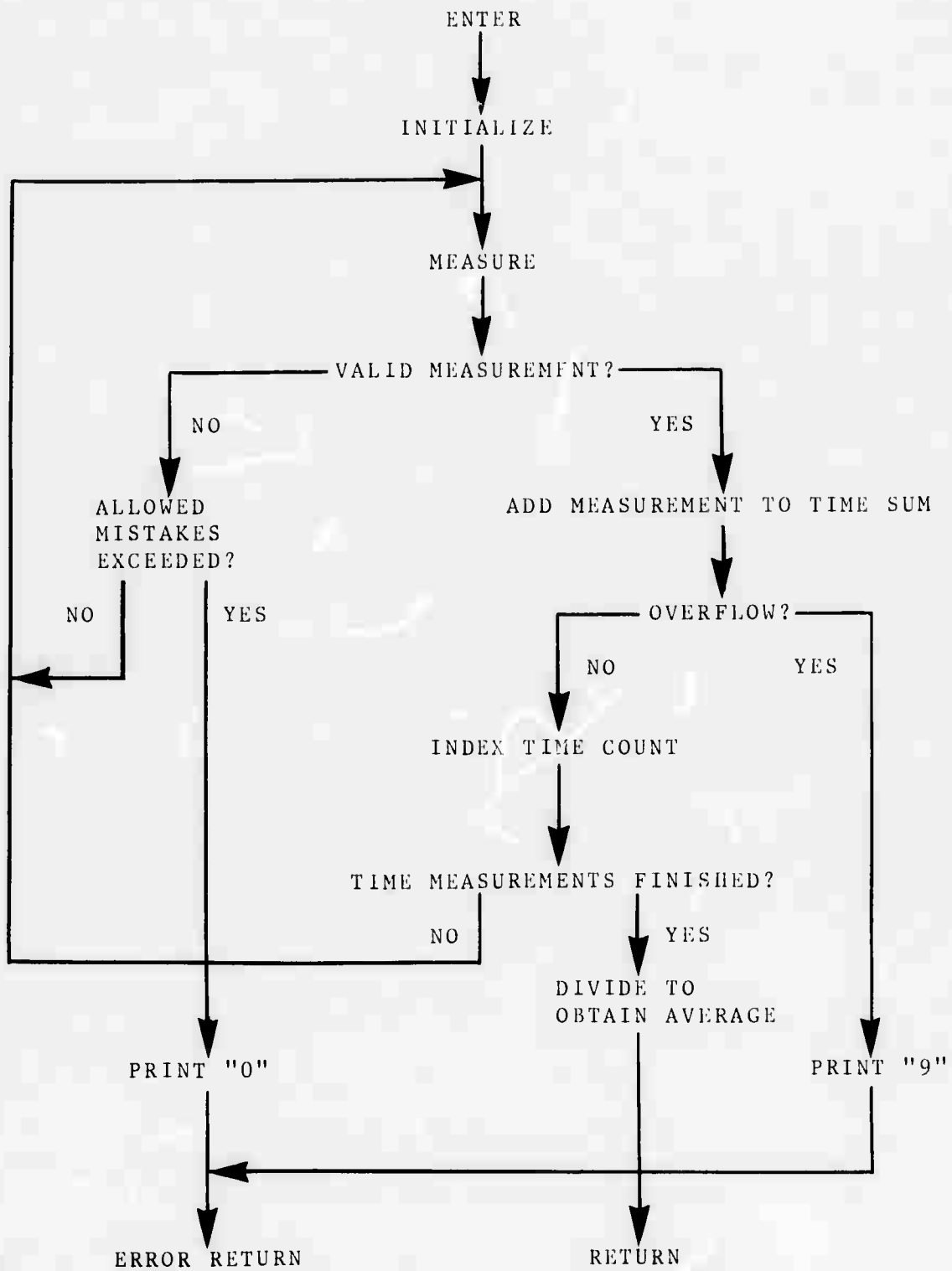

Figure 26. Flow Chart of TIME AVERAGE Subroutine

to a so-called time sum; a counter is indexed; and the next measurement is initiated. When the counter shows that the desired number of measurements have contributed to the time sum, this sum is divided by the number of measurements and the TIME AVERAGE subroutine returns with the resulting average measurement.

Note that invalid measurements (those where more or less than two edges are detected) are counted, and if more than the allowed number of mistakes are made, the subroutine signals the operator that a valid measurement could not be constructed within a reasonable number of attempts. Also, the TIME AVERAGE subroutine monitors the time sum and if it exceeds the capacity of the LINC accumulator, the operator is advised so that fewer measurements can be included in an average. In the future it may be profitable to use floating point numbers so that the chance of overflow will be lessened, but a reasonable number of measurements (eight to sixteen) may be included in an average with the present scheme without danger of overflow. Moreover, it is questionable whether the averages should be made big enough to necessitate floating point routines, since the amount of time required to repeatedly scan the measurement segment eventually begins to exceed the time taken by a dynamic image, such as that of a blood vessel, to change by a significant percentage. That is, the number of measurements in a time average must be carefully selected on the basis of known frequency and magnitude of changes in the physical distance being measured.

Whereas the philosophy of the time average is to reduce the effects of noise on the measured length, the reasoning behind the space average is to attempt to diminish the consequences of tiny irregularities in the input image itself. For instance, if a certain single measurement segment is chosen and it happens to include a small bump or notch in the outline, then the result is slightly too long or too short. But by averaging a series of measurements adjacent and parallel to the specified measurement segment, the final value is made more reliable because the little anomalies cancel each other.

Consider the flow chart of the SPACE AVERAGE subroutine in Figure 27. Although it is similar to the TIME AVERAGE subroutine, the significant difference is that in the SPACE AVERAGE subroutine the measurement segment is initially located to the left of the initially specified segment. After each valid time average measurement has been added to the running sum (here called the space sum), the measurement segment is moved one scan increment to the right. Calling the TIME AVERAGE subroutine for each measurement instead of calling for a single measurement is convenient because it allows any combination of space and time averages to be specified.

For instance, if the parameters which control the number of individual measurements in a time average and a space average are both four, then the procedure is to measure four times at the left end, add the resulting time average to the space sum, move one scan increment to the right, measure four more times and so on until four separate time averages have been added to the space sum. Then this sum is divided by four and the resulting number is typed out as the calculated dimension.

Reviewing the measurement routines, they afford methods of calibration and precise selection of measurement segments. Periodic measurements can be made under computer control. Time and space averages reduce the effects of electronic noise and image irregularities, respectively.

A number of minor extensions of the methods outlined above have been considered, but none has been implemented in the present system because of time limitations. One obvious possibility is to permit several simultaneous measurement segments; the computer would actually make measurements in each segment sequentially, but its speed makes this appear

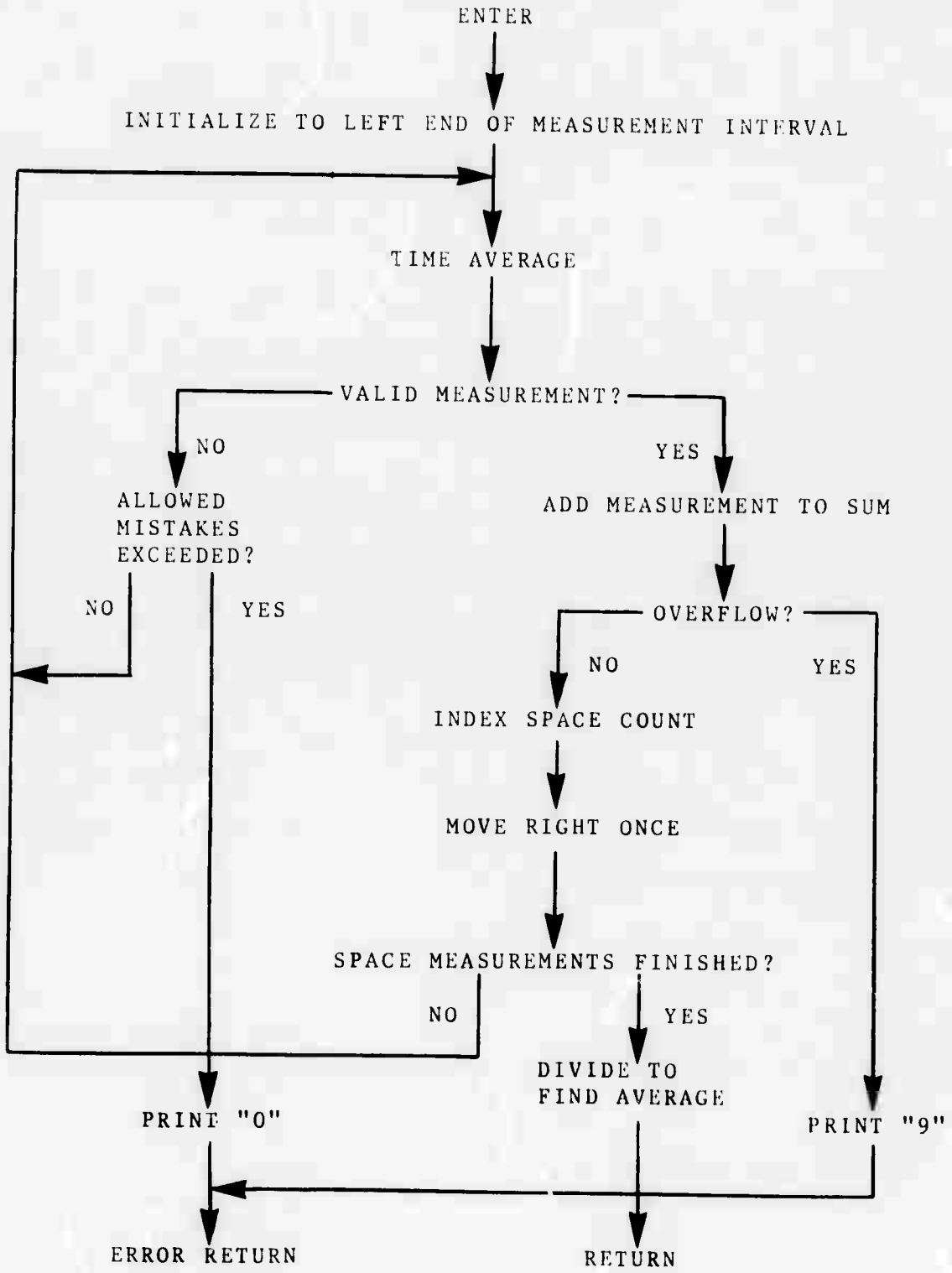

Figure 27. Flow Chart of SPACE AVERAGE Subroutine

nearly simultaneous. Another improvement is to measure at any angle in the picture; this could be accomplished by measuring on two parallel lines and using trigonometric identities to determine the intervening distance normal to the axis of the measured object. Still another proposal is to reject single measurements that differ radically from an accumulated average distance; this step would help reject any measurements whose endpoints are considerably affected by noise bursts. It is easy to see that all three of the extensions suggested are essentially founded upon the method already describing and working. Hence, it was deemed unnecessary and indeed unattractive to add the further steps to the experimental model of the device because further processing of the raw data makes it harder to interpret and harder to use in judging the performance of the basic method. Some typical results are therefore explained next.

5. RESULTS

Results of research using the system described in the previous chapters are explained under the classifications of outlines, measurements, and biological specimens. Only transformation AC is used in the examples, because best results to date have been obtained with AC (as shown in Chapter 3).

Effects of the threshold and averaging parameters on outline quality are summarized and also illustrated in several photographs. Experience has shown that raising any one of these parameters reduces the noise in the picture but also reduces the signal, so that a compromise is necessary.

Two sets of data are presented to elucidate the measurement procedure. Linearity and accuracy, important properties of a measurement system, are shown by the first set of data. Time and space averaged measurements are summarized by mean and standard deviation in the second set. In particular a given distance was repeatedly measured for many different combinations of time and space averaging and the resulting statistics are presented.

Finally, performance of the system in working with the mesoappendix of a live rat is considered. Halftone as well as outline photos of rat blood vessels are explained. A single line intensity trace demonstrates the amplitude of the signals involved.

5.1 OUTLINE RESULTS

Signal-to-noise ratio is of prime importance in the system reported here because the intensity data used in the automatic measurement operation is not filtered by a human. Humans are notorious for their ability to emphasize or ignore selected visual stimuli. Mach rings (See Chapter 2.) are a perfect example: gradual shadings are hardly perceived at all while a change in the rate of change of luminance with respect to distance appears as a well-defined edge. A more common instance of ignoring a stimulus is the way in which line noise, "snow," and various other distortions of television pictures can be overlooked by the casual viewer. These illustrations underline the point that since the machine has no such sophisticated processing, it is even more important to minimize the noise. If the signal is sufficiently larger than the noise, the noise will never be mistaken for the signal.

Accordingly, the parameters m, NC, and C are adjusted by the operator until they are optimum for each input image. In this section a transparency made from a magazine cover * is used to demonstrate the changes produced by the parameters mentioned. Figure 28(a) is a halftone picture of the cover produced by the image processing system. Note the wealth of detail that can be seen in the picture -- this detail makes the picture very challenging to scan for the purpose of producing outlines.

As more points are included in an average (i.e., as m increases), the waveform becomes smoother. Hence, the textures in the image contribute fewer edges to the outline output and this outline picture is usually easier to interpret because only the most obvious contours are detected. When m is increased, the thresholds may be lower without causing undue noise due to texture.

Figure 28(b) shows how the outline looks before m is increased. The same picture after 4-2 averaging was applied is shown in Figure 29(a), which is obviously a better picture with less noise.

Raising NC means that only the most rapidly changing parts of an input intensity profile contribute to edges considered by processor AC. Also the steepest parts of the curve tend to

*Forbes Magazine, Vol. 97, No. 3, February 1, 1966. Used with permission.

be the most stable and least susceptible to the type of noise which occurs near the ends of an edge and which will increase or decrease the length of the edge. Hence the contours produced are straighter than (i.e., not as notched as) contours produced using a lower NC. Also, isolated noise pulses are less often detected as edges with a high NC because such pulses typically have small amplitudes, which also limits the magnitude of their slope approximations.

The cleaner picture in Figure 29(b) results when NC was raised to 14 from its value of 10 in Figure 28(b). Note that raising either m or NC has a similar effect on the picture.

The third adjustment which can be made is to raise C, the cumulative threshold. Only an edge whose total amplitude between the NC cutoffs is equal to or greater than C will be detected when C > NC. C may be adjusted over a wide range because many of the important edges in most images have total amplitudes which are quite large. C is probably the most effective parameter for eliminating fine texture noise because such signals are quite small as compared to prominent edge signals.

Figure 29(c) shows the effect of raising C; it should be compared with Figure 28(b). Again, noise is reduced and the output image is easier to interpret.

Finally, increasing both NC and C from their values in Figure 28(b) yields the picture in part (d) of Figure 29. For some purposes the latter image is nearly optimum, but notice that some lines (for example, those in the left side of the man's neck) have disappeared entirely. Whether or not this loss is objectionable depends upon the interest of the observer. If the observer is attempting to recognize the outlines as representing a human face, the lines in the neck are probably unimportant and can be considered background noise. On the other hand an observer trying to determine the exact identity of the man may be considerably aided by seeing the neck lines.

5.2 MEASUREMENT RESULTS

Three important requirements are necessary in any length measurement tool: (a) it must be linear over its full range of input lengths, (b) the device must consistently report the same distance when the same dimension is repeatedly measured, and (c) it must report results to the required number of significant decimal places. If a system has these characteristics, it is relatively easy to compensate for most other failures. For example, if a constant offset is added to each measurement by the system, then it is easy to subtract this offset from each item of raw data before recording that item. Tests of accuracy and linearity as well as consistency are reported in this section.

First, the system described on these pages was tested for linearity and accuracy. The test pattern used is shown in Figure 30: there are sequential steps of distance from one to ten units in length between the opaque edges. After outlining the steps with transformation AC and calibrating with the longest distance (ten units), each step was measured forty times with the resulting mean taken as the measured dimension.

Results of the accuracy test are tabulated in Table 1. Arranged on the same line with each nominal value are two sets of measured lengths: the left set of four numbers refers to forty single measurements while the right set of four numbers refers to forty averaged measurements. Each of these averaged measurements is a combination of space and time averages; four single measurements are made on each of four parallel measurement segments (four time averages/space average and four single measurements/time average, or sixteen single measurements/averaged measurement). Thus a total of 6800 single measurements serve as the basis for the statistics presented. In each set the low and high values recorded by the system for

(a) Original Halftone Image

(b) Original Outline Image
(Averaging=2x2, NC=10, C=21)

Figure 28. Halftone Picture with Outline Before Parameter Adjustment

(a) Greater Averaging
[Averaging=4x2,
NC=10, C=21]

(b) Greater NC
[Averaging=2x2,
NC=14, C=21]

(c) Greater C
[Averaging=2x2,
NC=10, C=51]

(d) Greater NC and C
[Averaging=2x2,
NC=14, C=51]

Figure 29. Outline Images Showing Parameter Changes

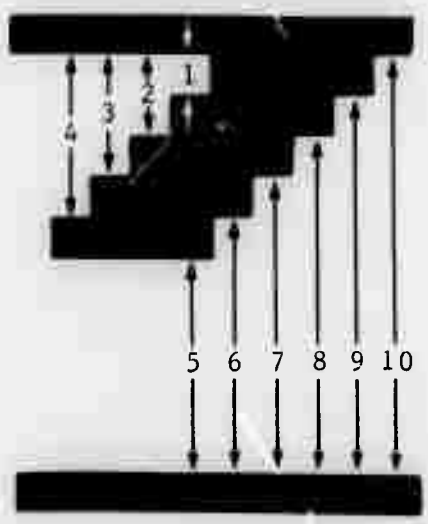

Figure 30. Measurement Accuracy Test Pattern

Table 1. Evaluation of Measurement Accuracy

NOMINAL LENGTH	MEASURED LENGTH							
	SINGLE MEASUREMENTS				AVERAGED MEASUREMENTS			
	LOW	HIGH	MEAN	STANDARD DEVIATION	LOW	HIGH	MEAN	STANDARD DEVIATION
1.0	1.00	1.06	1.05	0.022	1.00	1.06	1.03	0.011
2.0	2.00	2.00	2.00	0.000	1.98	2.03	2.00	0.011
3.0	2.89	3.01	2.95	0.032	2.92	2.95	2.93	0.013
4.0	3.84	3.95	3.92	0.031	3.87	3.92	3.89	0.014
5.0	4.95	5.01	4.96	0.020	4.98	5.01	4.99	0.013
6.0	5.96	5.96	5.96	0.000	5.93	5.96	5.96	0.008
7.0	6.90	6.96	6.90	0.010	6.90	6.93	6.90	0.007
8.0	7.85	7.90	7.88	0.013	7.88	7.90	7.89	0.009
9.0	8.79	8.91	8.85	0.043	8.82	8.85	8.83	0.014
10.0	9.80	9.85	9.80	0.014	9.80	9.82	9.81	0.010

each step are given to show the range and its relation to the nominal value. The mean value is computed on the basis of the forty measurements and stands as the distance computed by the system. Standard deviations are also included to show how the data clustered about the means.

As the table shows, the system is quite accurate and it is linear over the range of inputs. The largest error in the means as compared to the nominal lengths is 0.2 in the single measurement set for a nominal length of 10.0; this amounts to two percent of the measured distance. Ranges of the data have values from zero to 0.12; the largest range amounts to about one percent of the full calibration distance of ten. For the averaged measurements the greatest range is only 0.06. Note that (with the exception of the two anomalies for nominal lengths of two and six) the standard deviations for the averaged measurements are less than those for the single measurements. This underlines the value of the averaging operations.

Errors in these results are attributed primarily to quantization of the measured values. For example, the nominal length of 1.0 was measured as 1.00,as 1.03,and as 1.06 by the system. Since no values between these could be obtained, the slightest amount of noise was enough to change the measured value by 0.03. Small mistakes in positioning the calibration pointer as well as electronic noise in the system, unrelated intensity changes in the input image, and tiny irregularities in the measured pattern are other possible sources of error.

Next, a brief indication of the consistency of the system is given by Table 2. The measured object was a wedge-shaped piece cut out of black paper. It was measured 36 different times in each of 25 parameter settings, where each setting was a unique combination of time averaging and space averaging. That is, all possible combinations of space and time averages of 1, 2, 4, 10, and 20 (octal) measurements were used. Four bad measurements in either a time or space average were allowed before the further attempts were abandoned. An arbitrary calibration distance was set at 1000 as a convenient reference; therefore the measurements made are not absolute.

Each element in the matrix of Table 2 is identified by the number of single measurements in a time average at the left end of its row and the number of time averages in a space average at the top of its column. Moreover, each element consists of two entries: the top number is the mean of the 36 individual results for the particular combination of space and time averaging while the bottom number is the standard deviation of these measurements.

The results should be judged not so much on the agreement of the means throughout the tables as on the agreement of the means over a short period of time (i.e., throughout one set of 36 measurements, as reflected by their standard deviation). Nevertheless, the means have a range of only six for the entire table; this range amounts to only four percent of the middle value of 155.

As expected the standard deviations show a tendency to decrease as the number of single measurements in a time average or a space average increases. Numerically the standard deviation decreases by an average of 0.48 when the number of time averages in a space average is doubled; when the number of measurements in a time average is doubled, the average decrease in standard deviation is 0.47. Thus, on the basis of this small sample it appears that space averaging and time averaging are equally effective in influencing the consistency of the results. A number of cases may be found in the table where the standard deviation increases when the size of the average also increases. (For example, for one time measurement in each space average, an increase in the standard deviation from 2.01 to 2.20 results when the number of measurements in a time average increases from 4 to 10.) Errors of this type

Table 2. Evaluation of Measurement Consistency

FORMAT:

Mean
Standard Deviation

Number of Single Measurements in Each Time Average	Number of Time Measurements in Each Space Average				
	1	2	4	10	20
1	155.0 5.46	155.0 3.24	156.0 2.51	156.0 2.06	158.0 1.93
2	158.0 3.34	153.5 2.46	155.0 2.03	157.0 1.51	158.0 1.93
4	157.0 2.01	153.0 2.14	155.0 2.03	157.0 0.676	157.0 0.676
10	155.5 2.20	152.0 2.00	155.5 2.01	157.0 0.956	157.0 0.00
20	153.0 1.17	154.0 1.55	156.0 1.94	156.5 1.14	157.0 0.00

may be caused by the sources mentioned above for the first test. In addition the wedge-shaped piece of paper measured has slight anomalies which may have influenced the data.

In summary the measurement section of the programs is accurate, linear, and consistent. Although it is important to note that the tests described above measured between edges separating very dark and very light areas, this fact has little bearing on the results. If the measurements can be made between steep, long edges, they can also be made between shallow, short edges, though with less accuracy and consistency. Furthermore, the preprocessing circuitry, in addition to the digital method of contrast enhancement, allows edges to be lengthened and made steeper. Hence, the measurement routines are as good as the input data that contain the edges and the outline routine that detects the edges.

5.3 BIOLOGICAL RESULTS

Difficulties limiting optical resolution in viewing living organisms under magnification have been cited by Bloch: (a) conditions favorable to the tissues must be preserved in order to keep them alive, but these conditions do not provide maximum optical contrast; (b) the various parts of a living creature inherently have little contrast on the microscopic level; and (c) the field of view is not static but varies with an "...always present motion which varies in rate and amplitude and which is produced by the inherent contractibility of living tissue and the transmitted motions of the cardiac and respiratory systems" [16, pages 104-5]. All these obstacles have been encountered with the rat preparations used to test the performance of the system described in this work. In general, however, preliminary results of these biological tests have been encouraging. Several methods that have been developed for overcoming the resolution problem involved in viewing the blood vessels of the rat mesentery are explained next.

A compromise between tissue health and optical contrast was adopted by placing the anesthetized rat on a plastic platform which attaches to the microscope stage. Fluids which simultaneously keep the exposed tissues from drying and warm them are constantly dripped upon the preparation. This procedure ensures a tissue life of several hours and at the same time permits continuous viewing of the desired parts.

To provide greater contrast the intensities in the biological input image may be enhanced by either analog or digital means, monitored by the intensity line display. Another means of improving contrast that has been contemplated is the use of special optical filters to increase the intensity difference between points in the blood vessels and points in the surrounding tissue. Specifically, the vessels, which already appear dark to the camera, would be made to appear even darker by selectively attenuating the narrow band of light wavelengths which correspond to the color of the blood in the vessels. Although preliminary trials with such optical filters have not yielded significant improvements, this approach has not yet been eliminated from further study.

Peristalsis (involuntary contractions in the walls of hollow muscular structures) and the other tissue motions mentioned by Bloch have been observed in some of the preparations used to date. However, it now appears that the problem of motion is not as great as was feared when the research began: by carefully controlling the temperature and quantity of the fluid dripped on the mesentery, movement in the field of view can be almost eliminated. In order to ensure the high-quality performance required in a production system, it might be necessary to add another routine to the programs. This routine would establish several fiducial edges in the field of view at the beginning of a measurement session. Then the routine would again be

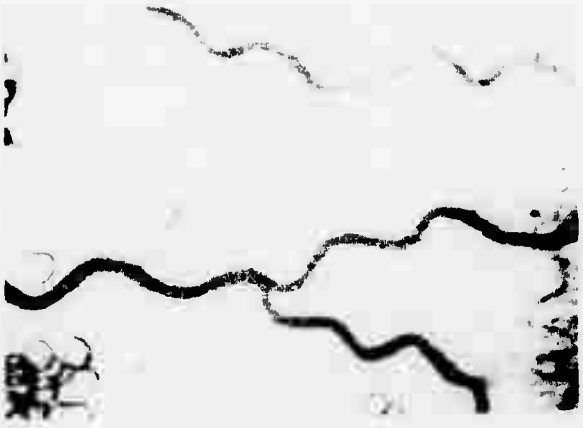

(a) Picture of Rat Mesentery Showing Blood Vessels and Fat Globules

(b) Corresponding Outline Image

(2x2, NC=10, C=30)

Figure 31. Halftone and Outline Images of Rat Mesentery

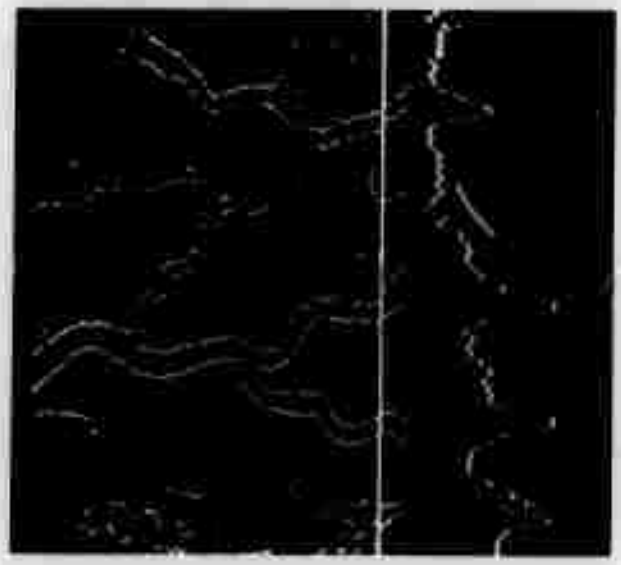

Figure 32. Blood Vessel Outlines with Typical Intensity Line Display

(2x2, NC=10, C=70)

Figure 33. Blood Vessel Outlines with Measurement Segment

(2x2, NC=10, C=30)

entered between measurements to check on these edges. If the edges had remained within a short distance of their previous locations, the measurements would proceed at once; otherwise, the routine would continue to check for the edges or to try to find them until the field of view was realigned with the fiducial edges before proceeding.

In a normal session with a rat about an hour is spent in making ready. During this period the physiologist anesthetizes the rat and makes an incision to expose its mesentery (the meso-appendix) which is placed under the microscope. At the same time the operator allows the equipment to warm up while making required adjustments of scope intensity, aspect ratio, and focusing. When the physiologist has selected the portion of the preparation to be viewed under the microscope (Figure 31(a)) is a typical field of view with the same image as an outline picture shown in Figure 31(b)), the preprocessing amplifiers are adjusted by the operator to permit full use of the input intensity range. Figure 32 shows a single trace of the rat vessels in one part of the outline. Intensity increases from right to left in the waveform along the right side of the picture, and the vertical intensified line marks the position for which the video waveform is shown. Note that the dark vessels are easily seen in the waveform as deep valleys.

After the fluid has been set to drip on the preparation, the system is calibrated for the measurements, the physiologist points out the vessels to be measured, and the system is put into the continuous measurement mode. The same area as in Figures 31 and 32 is shown in Figure 33 with a measurement segment specified by dots indicated by the white arrows. Note that the edges of the vessel appear thicker between the dots: this is due to small variations in the measured length over many measurements that accumulate to cause a short distance on each side of the original edge to be intensified. Thereafter the system continues to measure while a vasoactive substance is injected and begins to affect the vessel diameters. The tele-type output supplies a permanent record of these measurements for later analysis by the physiologist.

The photographs in this section show the capabilities of the outlining transformation as well as the procedures for measuring blood vessels. Comparison of the outlines in Figures 31, 32, and 33 with those in Figure 11 vividly demonstrates the improvement of the edge detection scheme from transformation SS to transformation AC. In the next chapter all the work on the system is summarized and various suggestions for extending the work are made, including recommendations for improving both the outlining and the measuring routines.

6. SUMMARY, CONCLUSIONS, AND EXTENSIONS

An existing on-line image processing system has been extended to measure distance between edges of objects in optical images. Such measurements are required for analyzing certain types of biological, metallurgical, and other visual data. Automatic measurement made possible by the system is especially useful when the measured distance changes as a function of time. Specifically, the system has successfully measured time-varying diameters of mesenteric blood vessels of live rats.

Particular advantages displayed by the system described here include low cost, flexibility, and speed. The image dissector camera, the processing transformations realized by the LINC, and the displays are all easily controlled, yet it is not difficult to modify them for new image processing applications. Any desired transformation of the multilevel input image can be programmed and experimentally tested on the LINC with relative ease. In addition, the ability to accept a comparatively wide range of input image formats and sizes is a definite advantage for various applications.

The concept of scanning the image as a two-dimensional read-only memory is also an important attribute of the system. Not only does this method permit economical use of memory by requiring only relatively small portions of the total picture to be in memory at one time, but it also keeps up-to-date information alway available on-line. This mode also permits more efficient man-machine interactions to take place with the aim of optimizing system performance.

Perhaps the largest limitation of the present system is the signal-to-noise ratio. Although a number of techniques (electronic filters, averaging methods, noise-suppressing transformations) have been used. the differential nature of the outline transformation continues to make it susceptible to noise.

Recommended extensions of this work fall naturally into two classes: (a) improvements of the outlining transformations and (b) improvements of the measurement routines. Certain changes in the existing transformations are easy to suggest. For example, AC could be modified to keep a short plateau from stopping one accumulation and starting another. Another possibility is the combination of certain aspects of the two processors; an outline point might be located at the steepest portion of an accumulation instead of at the middle, for instance. Finally, completely new transformations can be tried: applying a threshold to the second derivative of intensity with respect to distance, as Mach's work seems to suggest, is one example.

For some purposes the most important change that could be made in the measurement routines is to increase their precision. That is, the measured dimensions would be reported with more significant decimal places by processing the data with a modified version of transformation AC. Although the original specifications for the system, which call for accuracy on the order of ten percent, have been satisfied by the present device, it is believed that even better results could be obtained by making some rather major changes in AC.

Other extensions of the measurement routines could include the calculation of area by specifying a region containing an object and programming the system to sum the finite-width measured lengths. Another obvious improvement already mentioned in section 4.4 is to permit multiple measurement segments so that several distances in the picture could be measured almost simultaneously. Also discussed before is the addition of routines to measure in any desired direction in the image. These changes are not considered necessary to prove the system, but they are probably required for production runs. Others of a similar nature might be added according to the requests of the particular user.

7. BIBLIOGRAPHY

1. Chambers, R., and Zweifach, B.W., "Topography and Function of the Mesenteric Capillary Circulation," *American Journal of Anatomy*, Vol. 75, (173-205), 1944.
2. Mann, W.F., *Perceptual Process for Computers: Finding the Edges of a Polygon in the Field of View*, Computer Corporation of America Technical Report No. 10, March 22, 1966.
3. Ledley, R.S., and Ruddle, F.H., "Chromosome Analysis by Computer," *Scientific American*, Vol. 214, No. 4 (40-6), April 1966.
4. Ledley, R.S., Rotold, L.S., Gobal, T.J., Jacobsen, J.D., Ginsberg, M.D., and Wilson, J.B., "FIDAC: Film Input to Digital Automatic Computer and Associated Syntax-Directed Pattern-Recognition Programming System," *Optical and Electro-optical Information Processing*, J. Tippett, D. Berkowitz, L. Clapp, C. Koester, and A. Vanderburgh, Jr., (Eds.), The Massachusetts Institute of Technology Press, Cambridge, Massachusetts, 1965.
5. Jarrell-Ash Company, *Quantimet (QTM) TV-Analyzing Computer*, Jarrell-Ash Bulletin No. 2, September 1966.
6. Airborne Instruments Laboratory, *AIL Type 490 Flying Spot Microscanner*,(Sales Brochure), Airborne Instruments Laboratory, Deer Park, New York.
7. Airborne Instruments Laboratory, *AIL Type 491 Flying Spot Particle Analyzer*, (Sales Brochure), Airborne Instruments Laboratory. Deer Park, New York.
8. Kozlov, B.L., Kaminar, G.I., and Kuniskii, A.S., "Television Microscope for Studying Biological Structures in 248-700 nm Band," *Instruments and Experimental Techniques*, (925-9), July-August 1966.
9. Izzo, N.F., and Coles, W., "Blood-Cell Scanner Identifies Rare Cells," *Electronics*, Vol. 35, No. 17, (52-7), April 27, 1962.
10. Johnson, P.C., Hanson, K.M., Greatbatch, W.H., Jr., Gaebler, J., Cox, C., "Arteriolar Responses Studied in Vivo with a Flying Spot Microscope," *Federation Proceedings*, Vol. 24, No. 1, (334), January-February 1965.
11. Warner, L., and Brown, M.C., "Techniques for Studying Microcirculation in the Eye," *Anatomical Record*, Vol. 138, No. 4, (339), December 1960.
12. Van der Loos, H., and Glaser, E.M., "A Semi-Automatic Computer Microscope for Analysis of Neuronal Morphology," *Institute of Electrical and Electronics Engineers Transactions on Biomedical Engineering*, Vol. BME-12, No. 1, (22-31), January 1965.
13. Wiederhielm, C.A., "Transcapillary and Interstitial Transport Phenomena in the Mesentery," *Federation Proceedings*, Vol. 25, No. 4, (1789-98), November- December 1966.
14. Wiederhielm, C.A., "Continuous Recording of Arteriolar Dimensions with a Television Microscope," *Journal Applied Physiology*, Vol. 18, No. 5, (1041-2), September 1963.
15. Wiederhielm, C.A., "Distensibility Characteristics of Small Blood Vessels," *Federation Proceedings*, Vol. 24, No. 4, (1075-84), July-August 1965.
16. Bloch, E.H., "A Method for Studying the Dynamics of Transcapillary Transfer Quantitatively at the Microscopic Level *in situ* Living Organs," *Angiology*, Vol. 14, No. 3, (97-106), March 1963.
17. Baez, S., "Vascular Smooth Muscle: Quantitation of Cell Thickness in the Wall of Arterioles in the Living Animal *in situ*," *Science*, Vol. 159, No. 3814, (536-8), February 2, 1968.
18. Baez, S., "Recording of Microvascular Dimensions with an Image-splitter Television Microscope," *Journal of Applied Physiology*, Vol. 21, No. 1, (299-301), January 1966.
19. Clark, W.A., and Molnar, C.E., "A Description of the LINC," *Computers in Biomedical Research*, Stacy, R.W., and Waxman, B. (Eds.), Vol. 2, Academic Press, New York, (35-64),1965.

20. Clark, M.A., and Clark, W.A., *Programming the LINC*, Computer Research Laboratory, Washington University, St. Louis, Missouri, June 1965.
21. Guignon, J.E., Jr., and Kline, R.M., *Development of an On-line Image Processing System for the LINC*, Computer Systems Laboratory Technical Report No. 5, Washington University, St. Louis, Missouri, February 1968.
22. Mach, E., *The Analysis of Sensations*, translated by C.M. Williams and S. Waterlow, Open Court Publishing Company, Chicago, 1914.
23. Gibson, J., *The Perception of the Visual World*, Riverside Press, Cambridge, Massachusetts, 1950.
24. Attneave, F., and Arnoult, M.D., "The Qualitative Study of Shape and Pattern Perception," *Pattern Recognition: Theory, Experiment, Computer Simulations, and Dynamic Models of Form Perception and Discovery*, Uhr, L. (Ed.), John Wiley and Sons, Incorporated, New York, 1966.
25. Hurvich, L. and Jameson, D., *The Perception of Brightness and Darkness*, Allyn and Bacon, Incorporated, Boston, 1966.
26. Graham, C.H. (Ed.), *Vision and Visual Perception*, John Wiley and Sons, Incorporated, New York, 1965.
27. Attneave, F., "Some Informational Aspects of Visual Perception," *Psychological Review*, Vol. 61, No. 3, (183-93), May 1954.
28. Higgins, G.C., and Jones, L.A., "The Nature and Evaluation of the Sharpness of Photographic Images," *Journal of the Society of Motion Picture and Television Engineers*, Vol. 58, (277-90), 1952.
29. Brain, A.E., Macouski, A., Forsen, G.E., Baer, J.A., Childress, C.O., Novikoff, A.B., and Bourne, C.P., *Graphical-Data-Processing Study and Experimental Investigation*, Report No. 3, Stanford Research Institute, January 1961.
30. Clarke, A.B., *Photogrammetric Engineering*, Vol. 28, No. 3, (393-9), July 1962.
31. Class notes of author, Engineering 683, (Principles of Artificial Intelligence), Washington University, Spring 1968.
32. Minot, O.N., *Counting and Outlining of '2-dimensional' Patterns by Digital Computer*, U.S. Navy Electronics Laboratory Report Number TM-414, August 1960.
33. Private communication to author, July 4, 1967.
34. Roberts, L.G., "Machine Perception of Three Dimensional Solids," *Optical and Electro-optical Information Processing*, Tippet, J.T., Berkowitz, D.A., Clapp, L.C., Koester, C.J., and Vanderburgh, A., Jr. (Eds.), Massachusetts Institute of Technology Press, Cambridge, Massachusetts, Chapter 9, (159-197), 1965.
35. Huang, T.S., and Tretiak, O.J., "Research in Picture Processing," *Optical and Electro-optical Information Processing*, Tippet, J.T., Berkowitz, D.A., Clapp, L.C., Koester, C.J., and Vanderburgh, A., Jr. (Eds.), Massachusetts Institute of Technology Press, Cambridge, Massachusetts, Chapter 3, (45-57), 1965.
36. Brain, A.E., Duda, R.O., and Munson, J.H., *Graphical-Data-Processing Research Study and Experimental Investigation Report* No. 20, August 1965.
37. Rosenfeld, A., and Pfaltz, J.L., "Sequential Operations in Digital Picture Processing," *Journal of the Association of Computing Machinery*, Vol. 13, No. 4, (471-94), October 1966.
38. Schreiber, W.F., "Picture Coding," *Proceedings of the Institute of Electrical and Electronics Engineers*, Vol. 55, No. 3, (320-30), March 1967.

8. ACKNOWLEDGMENTS

We wish to express special thanks to the CSL staff and also to Dr. Stan Lang, Department of Physiology, Washington University School of Medicine, and to the first author's wife Elizabeth. The former labored to educate us in the wonders of things physiological and to assist us in tests of the system with live preparations, while the latter worked long hours drawing the final figures in this report.